and the aqueous layer was extracted with ether (5 × 10 mL). The combined organic layers were dried over $MgSO_4$ and concentrated. The crude product was subjected to flash chromatography (silica gel, 5% EtOAc/hexanes) to afford 210 mg of **68** (79%) as an amorphous solid: ^{1}H NMR ($CDCl_3$) δ 0.69 (3 H, $C_{18}CH_3$, s), 0.94 (3 H, $C_{21}CH_3$, d, $J \sim$ 6.8 Hz), 1.41 (6 H, C_32CH_3, s), 1.71 (3 H, $C_{27}CH_3$, s), 1.82 (3 H, $C_{19}CH_3$, s), 4.23 (2 H, br s), 4.27 (2 H, m), 4.67 (2 H, $2H_{26}$, br s), 5.93 (1 H, H_9, m).

Acknowledgment. This study was generously supported by the NIH Grant DK-16595, the UC Riverside Intramural Fund, and the Chancellor's Patent Fund. Duphar (Weesp, The Netherlands) provided generous quantities of vitamin D_3 utilized as starting material in this study. We also acknowledge Professor M. M. Midland for helpful discussions.

Supplementary Material Available: Spectral data for all new compounds and general experimental details (34 pages). Ordering information is given on any current masthead page.

Photoemission Probes of Hydrocarbon–DNA Interactions: A Comparison of DNA Influences on the Reactivities of (±)-*trans*-7,8-Dihydroxy-*anti*-9,10-epoxy-7,8,9,10-tetrahydrobenzo[*a*]pyrene, Benzo[*a*]pyrene 4,5-Oxide, and Benz[*a*]anthracene 5,6-Oxide

Shigeyuki Urano, Harry L. Price, Sharon M. Fetzer, Anita V. Briedis,† Ann Milliman, and Pierre R. LeBreton*

Contribution from the Department of Chemistry, The University of Illinois at Chicago, Chicago, Illinois 60680. *Received January 24, 1990. Revised Manuscript Received January 15, 1991*

Abstract: Time-resolved fluorescence and UV photoelectron measurements have been employed to examine the influence of calf thymus DNA on the reactivities of epoxides derived from benzo[*a*]pyrene (BP) and benz[*a*]anthracene (BA). By monitoring the increase in fluorescence intensity, which accompanies reaction at 23 °C, overall, pseudo-first-order rate constants have been measured for reactions of the highly carcinogenic bay region epoxide (±)-*trans*-7,8-dihydroxy-*anti*-9,10-epoxy-7,8,9,10-tetrahydrobenzo[*a*]pyrene (BPDE) and of two less carcinogenic K region epoxides benzo[*a*]pyrene 4,5-oxide (BPO) and benz[*a*]anthracene 5,6-oxide (BAO). Overall rate constants for hydrolysis and rearrangement reactions have been measured for BPDE, BPO, and BAO in buffer alone (1.0 mM sodium cacodylate, pH 7.1). The rate constants increase in the order BPO ($(3.8 \pm 0.1) \times 10^{-6}$ s^{-1}) < BAO ($(5.7 \pm 2.6) \times 10^{-5}$ s^{-1}) < BPDE ($(7.2 \pm 1.0) \times 10^{-4}$ s^{-1}). These results have been compared with overall rate constants for reactions, carried out in calf thymus DNA, which result in catalyzed hydrolysis and rearrangement, as well as DNA adduct formation. In DNA, the ordering of the rate constants for BPO and BAO changes from that observed in buffer alone. The rate constants increase in the order BAO ($(2.8 \pm 0.1) \times 10^{-3}$ s^{-1}) < BPO ($(1.2 \pm 0.2) \times 10^{-2}$ s^{-1}) < BPDE ($\sim 1 \times 10^{-1}$ s^{-1}). This ordering is the same as the ordering of association constants for the reversible binding to DNA of the fluorescent diols *trans*-7,8-dihydroxy-7,8-dihydro-BP (BP78D), *trans*-4,5-dihydroxy-4,5-dihydro-BP (BP45D) and *cis*-5,6-dihydroxy-5,6-dihydro-BA (BAD), which are model compounds of BPDE, BPO, and BAO, respectively. For the model compounds, the association constants for intercalation increase in the order BAD ($(3.6 \pm 0.9(\times 10^2$ M^{-1}) < BP45D ($(9.6 \pm 0.5) \times 10^3$ M^{-1}) < BP78D ($(3.4 \pm 0.1) \times 10^4$ M^{-1}). This ordering is consistent with the ordering of the association constants of BPDE ($(2.5 \pm 0.3) \times 10^4$ M^{-1}) and of BPO ($(6.0 \pm 1.0) \times 10^3$ M^{-1}). The temperature dependence of the association constants of the model compounds demonstrates that, for the intercalation of the BP diols into DNA, differences in the enthalpy of binding contribute significantly to differences in the free energy of binding. UV photoelectron data and results from ab initio molecular orbital calculations on BPDE, BPO, and BAO indicate that, for these three epoxides, the association constants increase as the ionization potentials decrease and the polarizabilities increase. The percentage of epoxide reaction that yields DNA adducts has been compared under varying conditions. For long reaction times (>1 h) in systems containing native, calf thymus DNA at low salt concentrations, the ordering of adduct yields is BPO (14.9 ± 1.1%) > BPDE (10.1 ± 3.0%) > BAO (3.6 ± 0.4%). For short reaction times (10 min) in systems containing native DNA stabilized with 0.10 mM Mg^{2+}, the ordering of adduct yields is BPDE (7.3 ± 1.9%) > BPO (1.3 ± 0.1%) > BAO (0.1 ± 0.1%). These results suggest that the ability of an epoxide to form adducts with exposed DNA during long reaction times is less indicative of the genotoxic potency of the epoxide than its ability to form adducts with stabilized DNA during short reaction times.

Introduction

Among the mutagenic and carcinogenic metabolites of benzo[*a*]pyrene (BP) and benz[*a*]anthracene (BA), the K region epoxides and the bay region diol epoxides have been the most carefully examined.[1-5] Early investigations of BP and BA metabolism focused on K region epoxides.[6-9] This interest shifted when cell cultures treated with parent hydrocarbons showed that major DNA adducts did not form from reactions of K region epoxides[7,10] but instead from reactions of bay region diol epoxides.[11]

†Current address: Department of Natural Science, Concordia College, River Forest, IL 60305.

(1) Phillips, D. H. *Nature* **1983**, *303*, 468.
(2) Conney, A. H. *Cancer Res.* **1982**, *42*, 4875.
(3) Koreeda, M.; Moore, P. D.; Yagi, H.; Yeh, H. J. C.; Jerina, D. M. *J. Am. Chem. Soc.* **1976**, *98*, 6720.
(4) Dipple, A.; Moschel, R. C.; Bigger, C. A. H. *Chemical Carcinogens*; Searle, C. E., Ed.; ACS Monograph Series 182; American Chemical Society: Washington, DC, 1984; Vol. 2, pp 41-163.
(5) Harvey, R. G. *Acc. Chem. Res.* **1981**, *14*, 218.

0002-7863/91/1513-3881$02.50/0

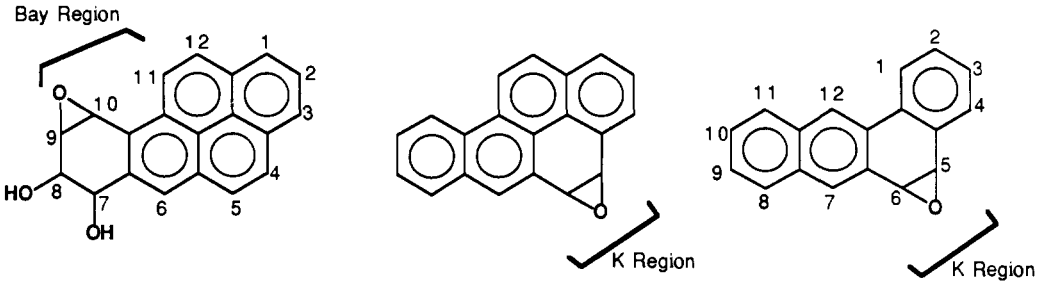

trans-7,8-dihydroxy-*anti*-9,10-epoxy-7,8,9,10-tetrahydrobenzo[a]pyrene (BPDE)

benzo[a]pyrene-4,5-oxide (BPO)

benz[a]anthracene-5,6-oxide (BAO)

Figure 1. Structures of the bay and K region epoxides (±)-*trans*-7,8-dihydroxy-*anti*-9,10-epoxy-7,8,9,10-tetrahydrobenzo[*a*]pyrene, benzo[*a*]pyrene 4,5-oxide, and benz[*a*]anthracene 5,6-oxide.

Structures of the bay region diol epoxide (±)-*trans*-7,8-dihydroxy-*anti*-9,10-epoxy-7,8,9,10-tetrahydrobenzo[*a*]pyrene (BPDE) and of the K region epoxides benzo[*a*]pyrene 4,5-oxide (BPO) and benz[*a*]anthracene 5,6-oxide (BAO), derived from BP and BA, are shown in Figure 1.

While different isomers of bay region diol epoxides exhibit different activity,[12,13] bay region metabolites are more mutagenic and carcinogenic than the K region epoxides.[10,14-16] Furthermore, benzo[*a*]pyrene and its most active metabolites are more genotoxic than benz[*a*]anthracene.[17,18] The varying biological activities of different epoxides derived from BP and BA, has been attributed to influences of π electronic structure on epoxide chemical reactivity.[14,15,19] Electronic considerations have led to the *bay region theory* of hydrocarbon carcinogenic activity, which predicts that the activities and the reactivities of bay region BP and BA diol epoxides are governed by the energy required to form carbonium ions. According to the theory, carbonium ions are reaction intermediates responsible for DNA modification. For BPDE, the primary DNA target site is the 2-amino group of guanine.[1,2,4,5,20] Frequently, the delocalization energy of the carbonium ion π system has been employed to gauge reactivity. The greater the delocalization energy, the greater is the predicted chemical reactivity and carcinogenic activity.

Predictions of the *bay region theory* correlate well with the genotoxic potency of BP and BA bay region diol epoxides.[15,19b,e,f,i] However, with the elucidation of details of BP and BA metabolism, it is becoming clear that other factors, such as susceptibility to enzymatic detoxification, also influence the activity of epoxides. For example, BPO and BAO are better epoxide hydrolase substrates than are the corresponding bay region diol epoxides.[21,22] Similarly, the reaction rate for the glutathione-*s*-transferase-catalyzed formation of glutathione conjugates is 4–5 times greater for BPO than for the BPDE precursor BP 7,8-oxide.[23] It is also likely that DNA adduct conformation,[24] the stability of DNA

(6) Grover, P. L.; Hewer, A.; Sims, P. *Biochem. Pharmacol.* **1972**, *21*, 2713.
(7) Baird, W. M.; Harvey, R. G.; Brookes, P. *Cancer Res.* **1975**, *35*, 54.
(8) Sims, P.; Grover, P. L. In *Advances in Cancer Research*; Klein, G., Weinhouse, S., Haddow, A., Eds.; Academic Press: New York, 1974; Vol. 20, pp 165–274.
(9) Grover, P. L.; Sims, P. *Biochem. Pharmacol.* **1973**, *22*, 661.
(10) Huberman, E.; Sachs, L.; Yang, S. K.; Gelboin, H. V. *Proc. Natl. Acad. Sci. U.S.A.* **1976**, *73*, 607.
(11) (a) Remsen, J.; Jerina, D.; Yagi, H.; Cerutti, P. *Biochem. Biophys. Res. Commun.* **1977**, *74*, 934. (b) Sims, P.; Grover, P. L.; Swaisland, A.; Pal, K.; Hewer, A. *Nature* **1974**, *252*, 326. (c) Grover, P. L.; Hewer, A.; Pal, K.; Sims, P. *Int. J. Cancer* **1976**, *18*, 1. (d) Jeffrey, A. M.; Weinstein, I. B.; Jennette, K. W.; Grzeskowiak, K.; Nakanishi, K. Harvey, R. G.; Autrup, H.; Harris, C. *Nature* **1977**, *269*, 348. (e) Shinohara, K.; Cerutti, P. A. *Proc. Natl. Acad. Sci. U.S.A.* **1977**, *74*, 979.
(12) (a) Levin, W.; Chang, R. L.; Wood, A. W.; Yagi, H.; Thakker, D. R.; Jerina, D. M.; Conney, A. H. *Cancer Res.* **1984**, *44*, 929. (b) Wood, A. W.; Chang, R. L.; Levin, W.; Yagi, H.; Thakker, D. R.; Jerina, D. M.; Conney, A. H. *Biochem. Biophys. Res. Commun.* **1977**, *77*, 1389.
(13) Kapitulnik, J.; Wislocki, P. G.; Levin, W.; Yagi, H.; Jerina, D. M.; Conney, A. H. *Cancer Res.* **1978**, *38*, 354.
(14) Jerina, D. M.; Lehr, R. E.; Yagi, H.; Hernandez, O.; Dansette, P. M.; Wislocki, P. G.; Wood, A. W.; Chang, R. L.; Levin, W.; Conney, A. H. In *In Vitro Metabolic Activation in Mutagenesis Testing*; de Serres, F. J., Fouts, J. R., Bend, J. R., Philpot, R. M., Eds.; Elsevier North-Holland Biomedical Press: Amsterdam, 1976; pp 159–177.
(15) Wood, A. W.; Levin, W.; Chang, R. L.; Yagi, H.; Thakker, D. R.; Lehr, R. E.; Jerina, D. M.; Conney, A. H. In *Polynuclear Aromatic Hydrocarbons*; Jones, P. W., Leber, P., Eds.; Ann Arbor Science Publishers, Inc.: Ann Arbor, MI, 1979; pp 531–551.
(16) (a) Wood, A. W.; Levin, W.; Lu, A. Y. H.; Ryan, D.; West, S. B.; Lehr, R. E.; Schaefer-Ridder, M.; Jerina, D. M.; Conney, A. H. *Biochem. Biophys. Res. Commun.* **1976**, *72*, 680. (b) Levin, W.; Wood, A. W.; Yagi, H.; Dansette, P. M.; Jerina, D. M.; Conney, A. H. *Proc. Natl. Acad. Sci. U.S.A.* **1976**, *73*, 243. (c) Kapitulnik, J.; Wislocki, P. G.; Levin, W.; Yagi, H.; Thakker, D. R.; Akagi, H.; Koreeda, M.; Jerina, D. M.; Conney, A. H. *Cancer Res.* **1978**, *38*, 2661.
(17) Slaga, T. J.; Huberman, E.; Selkirk, J. K.; Harvey, R. G.; Bracken, W. M. *Cancer Res.* **1978**, *38*, 1699.
(18) Wood, A. W.; Chang, R. L.; Levin, W.; Lehr, R. E.; Schaefer-Ridder, M.; Karle, J. M.; Jerina, D. M.; Conney, A. H. *Proc. Natl. Acad. Sci. U.S.A.* **1977**, *74*, 2746.
(19) (a) Jerina, D. M.; Daly, J. W. In *Drug Metabolism-from Microbe to Man*; Parke, D. V., Smith, R. L., Eds.; Taylor and Francis, Ltd.: London, 1977; pp 13–32. (b) Jerina, D. M.; Yagi, H.; Lehr, R. E.; Thakker, D. R.; Schaefer-Ridder, M.; Karle, J. M.; Levin, W.; Wood, A. W.; Chang, R. L.; Conney, A. H. In *Polycyclic Hydrocarbons and Cancer*; Gelboin, H. V., Ts'o, P. O. P., Eds.; Academic Press: New York, 1978; Vol. 1, pp 173–188. (c) Jerina, D. M.; Lehr, R. E. In *Microsomes and Drug Oxidations*; Ullrich, V., Roots, I., Hildebrandt, A., Estabrook, R. W., Eds.; Pergamon Press: Elmsford, NY, 1978; pp 709–720. (d) Smith, I. A.; Berger, G. D.; Seybold, P. G.; Servé, M. P. *Cancer Res.* **1978**, *38*, 2968. (e) Nordqvist, M.; Thakker, D. R.; Yagi, H.; Lehr, R. E.; Wood, A. W.; Levin, W.; Conney, A. H.; Jerina, D. M. In *Molecular Basis of Environmental Toxicity*; Bhatnagar, R. S., Ed.; Ann Arbor Science Publishers Inc.: Ann Arbor, MI, 1980; pp 329–357. (f) Lowe, J. P.; Silverman, B. D. *J. Am. Chem. Soc.* **1981**, *103*, 2852. (g) Thakker, D. R.; Yagi, H.; Nordqvist, M.; Lehr, R. E.; Levin, W.; Wood, A. W.; Chang, R. L.; Conney, A. H.; Jerina, D. M. In *Chemical Induction of Cancer*; Arcos, J. C., Woo, Y.-T., Argus, M. F., Eds.; Academic Press: New York, 1982; pp 727–747. (h) Sayer, J. M.; Lehr, R. E.; Whalen, D. L.; Yagi, H.; Jerina, D. M. *Tetrahedron Lett.* **1982**, *23*, 4431. (i) Lehr, R. E.; Kumar, S.; Levin, W.; Wood, A. W.; Chang, R. L.; Conney, A. H.; Yagi, H.; Sayer, J. M.; Jerina, D. M. In *Polycyclic Hydrocarbons and Carcinogenesis*; Harvey, R. G., Ed.; American Chemical Society: Washington, DC, 1985; pp 63–84.
(20) Weinstein, I. B.; Jeffrey, A. M.; Jennette, K. W.; Blobstein, S. H.; Harvey, R. G.; Harris, C.; Autrup, H.; Kasai, H.; Nakanishi, K. *Science (Washington, D.C.)* **1976**, *193*, 592.
(21) (a) Oesch, F. In *Enzymatic Basis of Detoxication*; Jakoby, W. B., Ed.; Academic Press: New York, 1980; Vol. 2, pp 277–290. (b) Bentley, P.; Schmassmann, H.; Sims, P.; Oesch, F. *Eur. J. Biochem.* **1976**, *69*, 97.
(22) Wood, A. W.; Levin, W.; Lu, A. Y. H.; Yagi, H.; Hernandez, O.; Jerina, D. M.; Conney, A. H. *J. Biol. Chem.* **1976**, *251*, 4882.
(23) Awasthi, Y. C.; Singh, S. V. *Biochem. Biophys. Res. Commun.* **1985**, *133*, 863.
(24) (a) Harvey, R. G.; Geacintov, N. E. *Acc. Chem. Res.* **1988**, *21*, 66. (b) Carberry, S. E.; Shahbaz, M.; Geacintov, N. E.; Harvey, R. G. *Chem.-Biol. Interact.* **1988**, *66*, 121. (c) Carberry, S. E.; Geacintov, N. E.; Harvey, R. G. *Carcinogenesis* **1989**, *10*, 97.

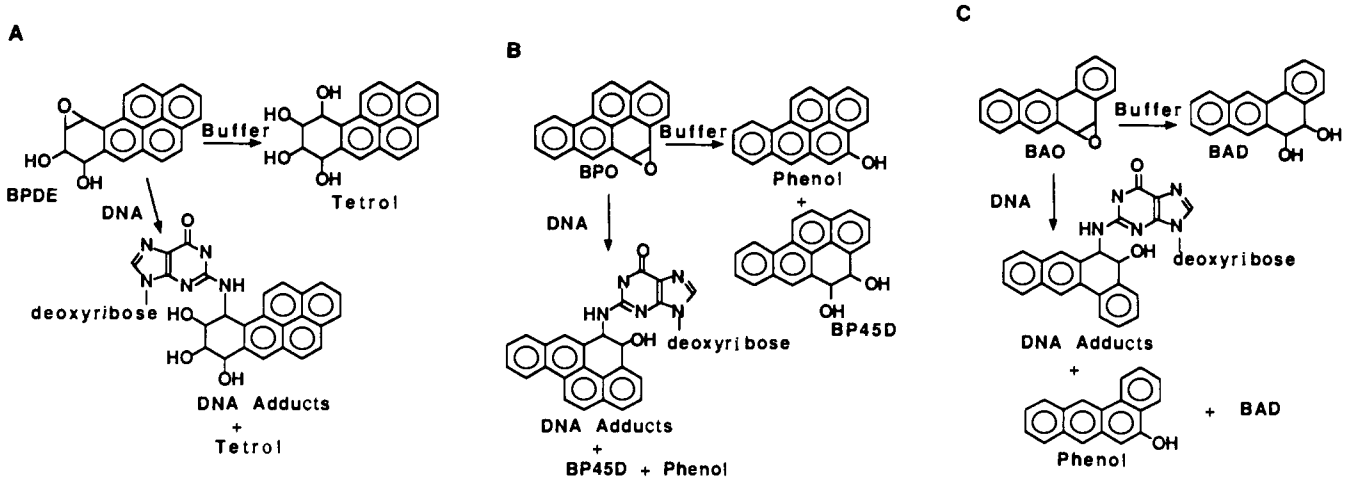

Figure 2. Major pathways for reactions of BPDE (A), BPO (B), and BAO (C) in buffer solutions and in solutions containing DNA.

adducts,[25] and the susceptibility of adducts to DNA repair mechanisms[26,27] influence the biological activities of hydrocarbon epoxides.

Relationship between Hydrocarbon Epoxide–DNA Physical Binding and Hydrocarbon Epoxide Reactivity. While covalent modification of nucleic acids by epoxides of BP and BA clearly is critical to genotoxic activity,[1-5] the significance of weaker physical binding interactions between DNA and BP and BA metabolites is uncertain.[28-37]

Investigations of mechanisms of epoxide reactions with nucleic acids demonstrate that intrinsic reactivity is not the sole factor, or in all cases the determinant factor, that governs the yield of DNA adducts. In vitro investigations of reactions of BPDE point out that, in addition to forming adducts, DNA catalyzes the hydrolysis of BPDE to 7,8,9,10-tetrahydro-BP.[28-32,38] In native DNA, the hydrolysis is accelerated 80 times.[31a] The observation that 5′-guanosine monophosphate catalyzes BPDE hydrolysis but that $H_2PO_4^-$ does not[39] suggests that stacking interactions between BPDE and nucleotide bases are important to catalysis.[40] Consistent with this conclusion are the observations that BPDE catalysis by DNA is reduced when the DNA is denatured or when reactions with native DNA are carried out with the DNA stabilizer Mg^{2+}.[29,31a] One interpretation of these results is that BPDE intercalation results only in DNA-catalyzed hydrolysis and leads only to detoxification.[41] Another interpretation is that mechanisms for BPDE hydrolysis and for DNA adduct formation involve similar transition states and that catalysis of hydrolysis is accompanied by autocatalysis of DNA covalent modification.[28,38]

Reactions of BPO and BAO with DNA have not been as carefully examined as those of BPDE. However, it is likely that, like BPDE, a major site of BPO adduct formation is the 2-amino group of guanine.[27,42] In addition to the formation of adducts, reactions of BPO with DNA and poly(guanylic acid) (poly(G)) result in a catalyzed hydrolysis to 4,5-dihydroxy-4,5-dihydro-BP and in a catalyzed rearrangement to the phenol 4-hydroxy-BP.[43]

Reactions of BAO[9] and of the related K region epoxides 7,12-dimethylbenz[*a*]anthracene 5,6-oxide[44] and phenanthrene 9,10-oxide[9] with poly(G) result in adduct yields that are about 5.4 times larger than yields with the corresponding uracil (poly(U)), cytosine (poly(C)), adenine (poly(A)), and inosine (poly(I)) homopolymers. Under acidic conditions, BAO undergoes rearrangement and hydrolysis.[45] These reactions, like those of BPO, are catalyzed by polynucleotides.[43] Figure 2 summarizes major pathways for reactions of BPDE, BPO, and BAO in buffered solutions and in buffered solutions containing DNA.[46]

This paper compares the reactivities of the three hydrocarbon epoxides shown in Figure 1. The comparison has been carried out by measuring overall, pseudo-first-order rate constants for reactions leading to adduct formation, rearrangement, and hydrolysis. Results of a comparison of the association constants for the reversible DNA binding of the nonreactive diols *trans*-7,8-

(25) Undeman, O.; Lycksell, P.-O.; Graslund, A.; Astlind, T.; Ehrenberg, A.; Jernstrom, B.; Tjerneld, F.; Norden, B. *Cancer Res.* **1983**, *43*, 1851.

(26) (a) Pelkonen, O.; Boobis, A. R.; Levitt, R. C.; Kouri, R. E.; Nebert, D. W. *Pharmacology* **1979**, *18*, 281. (b) Feldman, G.; Remsen, J.; Wang, T.-C. V.; Cerutti, P. *Biochemistry* **1980**, *19*, 1095.

(27) Rojas, M.; Alexandrov, K. *Carcinogenesis* **1986**, *7*, 235.

(28) Prakash, A. S.; Harvey, R. G.; LeBreton, P. R. In *Polynuclear Aromatic Hydrocarbons: A Decade Of Progress*; Cooke, M., Dennis, A. J., Eds.; Battelle Press: Columbis, OH, 1988; pp 699–710.

(29) MacLeod, M. C.; Selkirk, J. K. *Carcinogenesis* **1982**, *3*, 287.

(30) Geacintov, N. E.; Hibshoosh, H.; Ibanez, V.; Benjamin, M. J.; Harvey, R. G. *Biophys. Chem.* **1984**, *20*, 121.

(31) (a) Geacintov, N. E.; Yoshida, H.; Ibanez, V.; Harvey, R. G. *Biochemistry* **1982**, *21*, 1864. (b) Geacintov, N. E.; Shahbaz, M.; Ibanez, V.; Moussaoui, K.; Harvey, R. G. *Biochemistry* **1988**, *27*, 8380.

(32) (a) Michaud, D. P.; Gupta, S. C.; Whalen, D. L.; Sayer, J. M.; Jerina, D. M. *Chem.-Biol. Interact.* **1983**, *44*, 41. (b) MacLeod, M. C.; Zachary, K. *Chem.-Biol. Interact.* **1985**, *54*, 45. (c) MacLeod, M. C.; Zachary, K. L. *Carcinogenesis* **1985**, *6*, 147.

(33) Zegar, I. S.; Prakash, A. S.; Harvey, R. G.; LeBreton, P. R. *J. Am. Chem. Soc.* **1985**, *107*, 7990.

(34) Abramovich, M.; Prakash, A. S.; Harvey, R. G.; Zegar, I. S.; LeBreton, P. R. *Chem.-Biol. Interact.* **1985**, *55*, 39.

(35) LeBreton, P. R. In *Polycyclic Hydrocarbons and Carcinogenesis*; Harvey, R. G., Ed.; ACS Symposium Series 283; American Chemical Society: Washington, DC 1985; pp 209–238.

(36) Prakash, A. S.; Zegar, I. S.; Shahbaz, M.; LeBreton, P. R. *Int. J. Quantum Chem., Quantum. Biol. Symp.* **1983**, *10*, 349.

(37) (a) Shahbaz, M.; Harvey, R. G.; Prakash, A. S.; Boal, T. R.; Zegar, I. S.; LeBreton, P. R. *Biochem. Biophys. Res. Commun.* **1983**, *112*, 1. (b) Urano, S.; Fetzer, S.; Harvey, R. G.; LeBreton, P. R. *Biochem. Biophys. Res. Commun.* **1988**, *154*, 789.

(38) Meehan, T.; Bond, D. M. *Proc. Natl. Acad. Sci. U.S.A.* **1984**, *81*, 2635.

(39) Gupta, S. C.; Pohl, T. M.; Friedman, S. L.; Whalen, D. L.; Yagi, H.; Jerina, D. M. *J. Am. Chem. Soc.* **1982**, *104*, 3101.

(40) The exocyclic amino group on guanine has also been implicated in the catalysis of BPDE hydrolysis. This is supported by the observations that when reactions are run in synthetic polynucleotides, the ability to catalyze BPDE hydrolysis increases with increasing guanine–cytosine base pair content and that polydeoxyinosine–deoxycytidine is an ineffective catalyst for hydrolysis. See ref 32c.

(41) Chen, F-M. *Nucleic Acids Res.* **1983**, *11*, 7231.

(42) Jennette, K. W.; Jeffrey, A. M.; Blobstein, S. H.; Beland, F. A.; Harvey, R. G.; Weinstein, I. B. *Biochemistry* **1977**, *16*, 932.

(43) Murray, A. W.; Grover, P. L.; Sims, P. *Chem.-Biol. Interact.* **1976**, *13*, 57.

(44) Blobstein, S. H.; Weinstein, I. B.; Grunberger, D.; Weisgras, J.; Harvey, R. G. *Biochemistry* **1975**, *14*, 3451.

(45) Keller, J. W.; Heidelberger, C. *J. Am. Chem. Soc.* **1976**, *98*, 2328.

(46) In Figure 2, scheme B indicates that adduct formation occurs primarily via addition to the C_5 atom of BPO. This is consistent with the observation (ref 43) that BPO rearrangement, which like adduct formation proceeds through a transition state with significant carbocation character, results in the formation of 4-hydroxy-BP. Similarly, scheme C indicates that adduct formation occurs primarily via addition to the C_5 atom of BAO. This is consistent with the observation (ref 45) that rearrangement of BAO results in the formation of more 5-hydroxy- than 6-hydroxy-BA.

dihydroxy-7,8-dihydrobenzo[a]pyrene (BP78D), *trans*-4,5-dihydroxy-4,5-dihydrobenzo[a]pyrene (BP45D) and *cis*-5,6-dihydroxy-5,6-dihydrobenz[a]anthracene (BAD) are also given. Structures of BP45D and BAD are shown in Figure 2.

The epoxides BPDE, BPO, and BAO were chosen because both their reactivities and their association constants for intercalation into DNA vary significantly. A comparison of the reactive and physical binding interactions of these epoxides with DNA permits an assessment of the relationship between physical binding and reactivity.

Previous studies[29-31,47-49] of the physical binding of BPDE to DNA have relied primarily on UV absorption measurements. While it is possible to compare the association constants for BPDE and BPO via this method, absorption measurements of the physical binding of BAO to DNA are impeded by the strong overlap between the absorption spectra of BAO and DNA. The diols BP78D, BP45D, and BAD were chosen as model compounds for investigating DNA intercalation of BPDE, BPO, and BAO, respectively. The diols possess similar π electronic structure and many of the steric features of the epoxides. Furthermore, in contrast to the epoxides, the diols all exhibit high fluorescence quantum yields that facilitate reversible binding measurements.

Methods

General Procedures. Fluorescence emission spectra were measured with a Perkin-Elmer 650-10 fluorescence spectrometer. Magic angle fluorescence lifetime measurements employed a Photochemical Research Associates Model 2000 nanosecond fluorescence spectrometer equipped with aberration-corrected optics. A Glan polarizer was mounted on the excitation side and a film polarizer on the emission side. Ultraviolet absorption spectra were measured with a Cary 17 spectrometer. Samples used in fluorescence and absorption experiments were contained in 1-cm cells. Photoelectron spectra were obtained with a Perkin-Elmer PS-18 photoelectron spectrometer equipped with a heated probe and a HeI lamp.

Samples of BPDE, BPO, BAO, BP78D, BP45D, BAD, 4-hydroxy-BP, and 5-hydroxy-BA were purchased from the Midwest Research Institute through the NCI Chemical Carcinogen Repository. Standard samples of 7,8,9,10-tetrahydroxy-7,8,9,10-tetrahydro-BP (tetrol) were prepared by the hydrolysis of BPDE under mild conditions.[49] Calf thymus DNA was purchased from Worthington. Reagent-grade $MgCl_2$ from Aldrich was employed in experiments involving Mg^{2+}.

Measurements of rate constants, of association constants, and of DNA adducts were performed in a solvent system consisting of double-distilled water containing 1.0 mM sodium cacodylate (pH 7.1). These experiments were performed at a temperature of 23 ± 1 °C.

All kinetic and binding measurements were carried out at hydrocarbon concentrations in the range 10^{-6}–10^{-7} M. DNA concentrations are reported in terms of PO_4^- molarity calculated from absorption spectra and with use of the relationship that 0.15 mM PO_4^- equals one DNA A_{260} unit.[33,51] Experiments with Mg^{2+} were carried out at concentrations such that the Mg^{2+} charge matched the DNA phosphate charge.

The DNA used here contained less than 1.2% protein. In control experiments, DNA obtained from the supplier was purified by using a phenol–chloroform extraction procedure,[52] which yielded an A_{260}/A_{280} ratio of 1.9. When Stern–Volmer quenching constants for BP78D were compared by use of purified DNA and DNA directly from the supplier, the difference was less than 10%. Subsequent experiments were carried out without purification. Denatured DNA was prepared by heating native DNA to 95 °C for 5 min followed by rapid cooling in ice–water. At 260 nm, the denatured DNA exhibited a hyperchromicity of 30%.

Overall, Pseudo-First-Order Reaction Rate Constants. In the kinetic experiments, pseudo-first-order rate constants for reactions leading to adduct formation, hydrolysis, and rearrangement were monitored by measuring the increase in the fluorescence emission intensity that accompanies product formation. The epoxides have negligible fluorescence quantum yields compared to the reaction products.[30] In the present experiments, the fluorescence emission intensities, extrapolated to the time at which the reactions were initiated, were less than 5% of the intensities observed at the completion of the reactions. The excitation wavelengths used in the kinetics experiments were 350, 330, and 310 nm for BPDE, BPO, and BAO, respectively. The emission wavelengths were 404, 388, and 368 nm.

The kinetic experiments were initiated by injecting 20 μL of a tetrahydrofuran solution containing one of the epoxides into 1 mL of solvent. The epoxide concentration employed in each experiment was obtained from UV absorption measurements by utilizing the extinction coefficient provided by the supplier. In kinetics experiments with DNA, the PO_4^- concentration was 0.20 mM. Pseudo-first-order rate constants were obtained by using a previously described method.[36] The rate constants are equal to minus the slopes of least-squares linear fits of plots of ln $[(I_{max} - I(t))/(I_{max} - I_0)]$ versus t. Here, I_{max} is the emission intensity of the reaction system measured after the reaction was completed, $I(t)$ is the intensity at time t, and I_0 is the fluorescence intensity of the system when the reaction was initiated.

Adduct Yields. The percentage of epoxide reaction leading to DNA adduct formation was measured by separating the DNA adducts from products of side reactions leading to hydrolysis and rearrangement. These experiments were run under the same conditions as the kinetics experiments, except that the volume of the reaction system was increased to 5 mL. The separation of DNA adducts from side products employed a method similar to that developed previously.[3] After a 24-h reaction time, the hydrolysis and rearrangement products were extracted from the reaction mixture with a buffer-saturated ethyl acetate solution (5 mL × 3) and 2 drops of concentrated HCl were added to the aqueous layer, which contained modified DNA. The covalently bound hydrocarbon adducts were then hydrolyzed by boiling for 1 h. After cooling, the hydrolyzed hydrocarbon adducts were recovered: BPDE as the tetrol and BPO and BAO as the diols BP45D and BAD, respectively. The recovery was carried out by combining successive extractions made with 5, 3, and 2 mL of ethyl acetate.

Quantification of adducts was carried out by comparing the fluorescence intensity of the ethyl acetate solution containing tetrol, BP45D, or BAD, obtained from hydrolysis of the modified DNA, with a standard solution of tetrol, BP45D, or BAD.

In two sets of control experiments, the procedure employed here was tested in order to eliminate the possibility that error was introduced by hydrocarbon loss during DNA hydrolysis. In one set of experiments, the DNA adducts were hydrolyzed, in the pH range 1.4–1.9, at temperatures of 80–90 °C, for 1–1.5 h in sealed vials. Under these conditions, the results were the same, within 1 standard deviation, as results obtained via the procedure described above. When the hydrolysis reaction times were increased, the results remained unchanged. The second set of control experiments, also run in closed vials, was used to test the stability of tetrol, BP45D, and BAD under hydrolysis conditions. In these experiments, samples of tetrol, BP45D, and BAD were added to acidic solution and heated for 1–1.5 h. The emission spectra of the heated samples were then compared to emission spectra of unheated samples to which acid was added immediately prior to fluorescence measurements. The emission intensities of the heated and the unheated samples were found to be equal to within 10%.

In a further test to determine whether acid hydrolysis altered the DNA fluorescence properties, the fluorescence emission spectra of a DNA sample, which was subjected to the hydrolysis procedure, was compared to the fluorescence emission spectrum of an untreated DNA sample. At the excitation and emission wavelengths employed in this investigation, the emission intensities of the two samples were identical.

DNA Fluorescence Quenching Constants for BP78D, BP45D, and BAD. Stern–Volmer plots were measured for BP78D, BP45D, and BAD at the same excitation and emission wavelengths used to monitor the reaction kinetics of the corresponding epoxides BPDE, BPO, and BAO. Quenching constants (K_{sv}) are equal to the slopes of least-squares fits to plots of I_0/I versus the DNA concentration. Here, I_0 corresponds to the fluorescence emission intensity of hydrocarbon without DNA and I corresponds to the intensity with DNA.

Fluorescence Lifetimes of BP78D, BP45D, and BAD. Fluorescence lifetime measurements of BP78D, BP45D, and BAD were carried out at the same excitation and emission wavelengths as used in the fluorescence quenching measurements. The quenching of the diol fluorescence by DNA required that, in measurements with DNA, a subtraction procedure be employed to correct for scattered light. In this procedure, the decay profile of a DNA blank was subtracted from the profile measured for a diol with DNA. Lifetime measurements with DNA were carried out at PO_4^- concentrations of 0.10, 0.20, and 0.50 mM for BP78D, BP45D, and BAD, respectively. The more weakly quenched diols BP45D and BAD

(47) Meehan, T.; Gamper, H.; Becker, J. F. *J. Biol. Chem.* **1982**, *257*, 10479.
(48) Geacintov, N. E.; Yoshida, H.; Ibanez, V.; Harvey, R. G. *Biochem. Biophys. Res. Commun.* **1981**, *100*, 1569.
(49) MacLeod, M. C.; Smith, B.; McClay, J. *J. Biol. Chem.* **1987**, *262*, 1081.
(50) Wolfe, A.; Shimer, G. H.; Meehan, T. *Biochemistry* **1987**, *26*, 6392.
(51) Ibanez, V.; Geacintov, N. E.; Gagliano, A. G., Brandimarte, S.; Harvey, R. G. *J. Am. Chem. Soc.* **1980**, *102*, 5661.
(52) Maniatis, T.; Fritsch, E. F.; Sambrook, J. *Molecular Cloning a Laboratory Manual*; Cold Spring Harbor Laboratory: Cold Spring Harbor, 1982; pp 458–460.

were examined at higher DNA concentrations than BP78D. Analysis of the lifetime data was performed with use of a least-squares deconvolution method.[53]

Temperature Dependence of Diol Association Constants. Values of the changes in enthalpy (ΔH) and entropy (ΔS) resulting from the binding of BP78D, BP45D, and BAD to native, calf thymus DNA have been obtained by measuring the temperature dependence of association constants (K_A's) determined from Stern–Volmer quenching constants. Values of ΔH and ΔS have been obtained from a least-squares linear fit to van't Hoff plots of ln K_A versus $1/T$.[54] Association constants were measured at temperatures of 15, 20, 25, 30, and 35 °C. For BP78D and BP45D, the association constants were measured at a DNA concentration of 0.20 mM; for BAD, the concentration was 0.50 mM. The excitation and emission wavelengths employed were the same as those used in the fluorescence lifetime measurements.

Association Constants for the Reversible Binding of BPDE and BPO to DNA. Association constants of BPDE and BPO were obtained by monitoring differences between the UV absorption spectrum of the free hydrocarbon and of the hydrocarbon–DNA complex.[29] Experiments were initiated by injecting 30 μL of a tetrahydrofuran (THF) solution containing BPDE or BPO into 1470 μL of a solution containing native, calf thymus DNA. Different DNA concentrations (between 0.00 and 0.50 mM) were employed. The reference cell contained the same solution as the sample cell, except for the hydrocarbon.

Binding measurements were performed in 1.0 mM sodium cacodylate adjusted to a pH of 9.0 by adding NaOH. A high pH was used to minimize hydrolysis and rearrangement reactions. At a pH of 9.0, the catalytic effect of DNA is negligible.[30] When solutions were monitored 30 s after BPDE or BPO was injected, less than 5% reaction occurred, even at the highest DNA concentrations used.

At 25 s after the addition of BPDE or BPO, the absorbance was measured at the wavelength ($\lambda_{complex}$) at which the DNA–hydrocarbon epoxide complex has an absorption maximum. For complexes of BPDE and BPO, $\lambda_{complex}$ occurs at 354 and 333 nm, respectively. After 35 s, the absorbance was measured at the wavelength (λ_{free}) at which the free hydrocarbon epoxide has an absorption maximum. For BPDE and BPO, λ_{free} occurs at 345 and 325 nm.

In separate experiments, absorbance measurements at λ_{free} were made every 5 s after the addition of BPDE and BPO to each of the DNA solutions. These measurements provided calibration curves that were used to calculate λ_{free} absorbances, 25 s after the addition of each epoxide, from λ_{free} absorbances, measured at 35 s.

Photoelectron Spectra. Photoelectron spectra of BPDE, BPO, and BAO were measured at temperatures of 176, 138, and 122 °C, respectively. Vertical ionization potentials were obtained from spectra calibrated to the $^2P_{3/2}$ and $^2P_{1/2}$ bands of Ar and Xe. At the temperatures employed, spectra of BPDE, BPO, and BAO, monitored for a period of 1 h, remained constant and showed no signs of decomposition. In order to further test whether decomposition occurred under the conditions of these experiments, high performance liquid chromatography was used to examine samples before and after spectra were measured. A Beckman Model 420 chromatograph with a Du Pont Zorbox SIL silica gel column was used. Samples were eluted with a THF/hexane (30/70) solvent system. Control experiments were carried out to verify that the HPLC method employed is capable of separately detecting 4-hydroxy-BP in the presence of BPO and 5-hydroxy-BA in the presence of BAO. An examination of chromatograms obtained from samples after they were removed from the photoelectron spectrometer indicated that the precent decomposition was 5% or less.

Molecular Orbital Calculations. Ab initio SCF molecular orbital calculations were carried out by employing the STO-3G, 4-31G, 4-31G*, 6-31G, and 6-31G* basis sets.[55-58] The calculations were performed on CRAY X-MP/48, IBM 3090/200 E/VF, and IBM 3090/600 E/VF computers by using the Gaussian 86[59] and 88[60] programs.

Table I. Wavelengths[a] of Maximum Intensity in Uncorrected Emission Spectra[b]

Extracted Reaction Products[c]

reactant	excitation wavelength	wavelengths of maximum emission intensity: without DNA[d]	with DNA[e]
BPDE	350	402	402
BAO	274	353	353, ~425
BPO	280	372, 390, 425	372, 390, 425

Standards

molecule	excitation wavelength	wavelengths of maximum emission intensity
7,8,9,10-tetrahydroxy-7,8,9,10-tetrahydrobenzo[*a*]pyrene (tetrol)	350	402
trans-5,6-dihydroxy-5,6-dihydrobenz[*a*]anthracene (BAD)	274	353
5-hydroxybenz[*a*]anthracene	274	430
trans-4,5-dihydroxy-4,5-dihydrobenzo[*a*]pyrene (BP45D)	280	372, 390
4-hydroxybenzo[*a*]pyrene	280	427

[a] All wavelengths in nanometers. [b] Spectra measured in ethyl acetate. [c] Products extracted from reaction mixtures with ethyl acetate. [d] Reactions run in buffer without DNA. [e] Reactions run in buffer with DNA.

For the calculations, geometries of BPDE and BPO were taken from crystallographic data.[61,62] For BPO, the crystal data yields anomalously small sp^3 C–H bond lengths, which average 0.94 Å. For calculations on BPO, the sp^3 C–H bond lengths were increased to 1.06 Å. This is the average value occurring in BPDE. The geometry of BAO was obtained by combining the crystal structure of phenanthrene 9,10-oxide with the structure of benzene.[63,64]

Results

Emission Characteristics of Products Formed in Hydrolysis and Rearrangement Reactions of BPDE, BPO, and BAO. Table I lists wavelengths of maximum emission in uncorrected emission spectra. The spectra were measured for solutions containing products extracted, with ethyl acetate, from reactions of BPDE, BAO, and BPO run with and without DNA. Spectra were also measured for standard samples of tetrol, BAD, 5-hydroxy-BA, BP45D, and 4-hydroxy-BP.

When BPDE reacts in buffer containing DNA, the fraction of products that can be extracted with ethyl acetate includes all products except the DNA adducts. This fraction exhibits a fluorescence spectrum identical with that of tetrol. At an excitation wavelength of 350 nm, the emission spectra of the extracted product formed in the reaction of BPDE with DNA and the standard tetrol sample both exhibit a maximum at 402 nm.

When BAO reacts in buffer alone, the emission spectrum of the extracted product has a maximum at the same wavelength (353 nm) as the maximum in the spectrum of the BAD standard. When BAO reacts in buffer containing DNA, the fluorescence spectrum of the extracted product fraction is more complicated than that observed in reactions occurring in buffer alone. At an excitation wavelength of 274 nm, the emission spectra of the extracted products have maxima at 353 and ~425 nm. These maxima occur at wavelengths that are characteristic of products

(53) Hui, M. H.; Ware, W. R. *J. Am. Chem. Soc.* **1976**, *98*, 4718.
(54) (a) Fried, V.; Hameka, H. F.; Blukis, U. *Physical Chemistry*; Macmillan: New York, 1977; pp 257–259. (b) Skoog, D. A.; West, D. M.; Holler, F. J. *Fundamentals of Analytical Chemistry*; Saunders College: Chicago, 1988; pp 40–44.
(55) Hehre, W. J.; Ditchfield, R.; Stewart, R. F.; Pople, J. A. *J. Chem. Phys.* **1970**, *52*, 2769.
(56) Ditchfield, R.; Hehre, W. J.; Pople, J. A. *J. Chem. Phys.* **1971**, *54*, 724.
(57) Hehre, W. J.; Ditchfield, R.; Pople, J. A. *J. Chem. Phys.* **1972**, *56*, 2257.
(58) Hariharan, P. C.; Pople, J. A. *Theor. Chim. Acta* **1973**, *28*, 213.
(59) The Gaussian 86 program was obtained from Carnegie-Mellon University and written by Binkley, J. S.; Frisch, M. J.; Raghavachari, K.; DeFrees, D.; Schlegel, H. B.; Whiteside, R.; Fluder, E.; Seeger, R.; Fox, D. J.; Head-Gordon, M.; and Topiol, S.
(60) Gaussian 88: Frisch, M. J.; Head-Gordon, M.; Schlegel, H. B.; Raghavachari, K.; Binkley, J. S.; Gonzalez, C.; Defrees, D.; Fox, D. J.; Whiteside, R. A.; Seeger, R.; Melius, C. F.; Baker, J.; Martin, R.; Kahn, L. R.; Stewart, J. J. P.; Fluder, E. M.; Topiol, S.; Pople, J. A. Gaussian Inc.: Pittsburgh, PA, 1988.
(61) Neidle, S.; Subbiah, A.; Cooper, C. S.; Riberio, O. *Carcinogenesis* **1980**, *1*, 249.
(62) Glusker, J. P.; Zacharias, D. E.; Carrell, H. L.; Fu, P. P.; Harvey, R. G. *Cancer Res.* **1976**, *36*, 3951.
(63) Glusker, J. P.; Carrell, H. L.; Zacharias, D. E.; Harvey, R. G. *Cancer Biochem. Biophys.* **1974**, *1*, 43.
(64) Bowen, H. J. M.; Donohue, J.; Jenkin, D. G.; Kennard, O.; Wheatley, P. J.; Whiffen, D. H. In *Tables of Interatomic Distances and Configuration in Molecules and Ions*; Sutton, L. E., Jenkin, D. G., Mitchell, A. D., Cross, L. C., Eds.; The Chemical Society: London, 1958; p M 196.

Table II. Pseudo-First-Order Reaction Rate Constants[a,b]

	buffer	native DNA[c]	denatured DNA[c]	native DNA + Mg^{2+} [c,d]
BPDE	$(7.2 \pm 1.0) \times 10^{-4}$	$\sim 1 \times 10^{-1}$	$(1.1 \pm 0.1) \times 10^{-2}$	$(4.7 \pm 2.7) \times 10^{-3}$
BPO	$(3.8 \pm 0.1) \times 10^{-6}$	$(1.2 \pm 0.2) \times 10^{-2}$	$(2.8 \pm 0.7) \times 10^{-4}$	$(2.0 \pm 0.6) \times 10^{-4}$
BAO	$(5.7 \pm 2.6) \times 10^{-5}$	$(2.8 \pm 0.1) \times 10^{-3}$	$(1.7 \pm 0.2) \times 10^{-4}$	$(9.2 \pm 0.3) \times 10^{-5}$

[a] In inverse seconds. [b] Measured in 1.0 mM sodium cacodylate (pH 7.1). [c] Measured in calf thymus DNA at a concentration of 0.20 mM in PO_4^-. [d] Measured at an Mg^{2+} concentration of 0.10 mM.

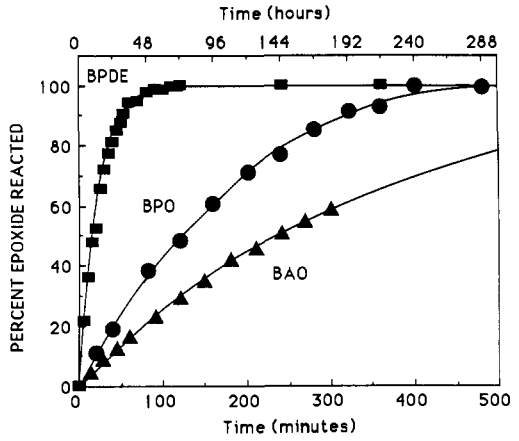

Figure 3. Results of kinetic measurements of overall, pseudo-first-order rate constants for reactions of BPDE (■), BAO (▲), and BPO (●) in 1.0 mM sodium cacodylate. The time scale at the bottom refers to data for BPDE and BAO. The time scale at the top refers to data for BPO.

formed in the hydrolysis reaction leading to BAD and in the rearrangement reactions leading to 5-hydroxy- and 6-hydroxy-BA. At an excitation wavelength of 274 nm, the emission spectrum of 5-hydroxy-BA has a maximum at 430 nm.

When BPO reacts both in buffer alone and in buffer containing DNA the ethyl acetate extract contains products of both BPO hydrolysis and rearrangement. Both with and without DNA, the extracted product emission spectrum has maxima that correspond to maxima in the emission spectra of BP45D and of 4-hydroxy-BP.

The present results agree with the conclusion that, with DNA, BPDE hydrolysis is the only major reaction that occurs, other than those leading to DNA modification.[28-32,39] They are also consistent with reports[43,45,65] that, in aqueous solution, K region epoxides form both hydrolysis and rearrangement products. In a 1/1 dioxane/water solvent system (pH 6.3), BAO yields 33% dihydrodiols and 67% phenols. Of the diols, 31% are in the cis form. Of the total phenol yield, 60% is 5-hydroxy- and 40% is 6-hydroxy-BA.[45] The reaction of phenanthrene 9,10-oxide in 67% acetone (pH 2.4) yields 17% *trans*-9,10-dihydroxy-9,10-dihydrophenanthrene and 75% 9-hydroxyphenanthrene.[65] In the present experiments, which were carried out near neutral pH in a more polar solvent system, the yields of phenols are significantly lower than those reported above. Without DNA, phenol formation was observed for BPO but not for BAO.

Effects of Calf Thymus DNA on Overall, Pseudo-First-Order Rate Constants of BPDE, BPO, and BAO. Figure 3 shows results of fluorescence intensity measurements of the percentage of BPDE, BPO, and BAO that has reacted, in aqueous buffered solution, as a function of time. In Figure 3, the fluorescence intensity of each hydrocarbon, measured at a given time, has been normalized to the intensity measured when the reaction is completed. Table II lists overall, pseudo-first-order rate constants. The results in Table II demonstrate that, in cacodylate buffer, the rate constants increase in the order

$$\text{BPO} < \text{BAO} < \text{BPDE}$$

and that the ratio of the rate constants is 1/15/190. The data in Figure 3 is in general agreement with the *bay region theory*,[14,15,19] which predicts that reactivity is greater for BPDE than for BAO or BPO.

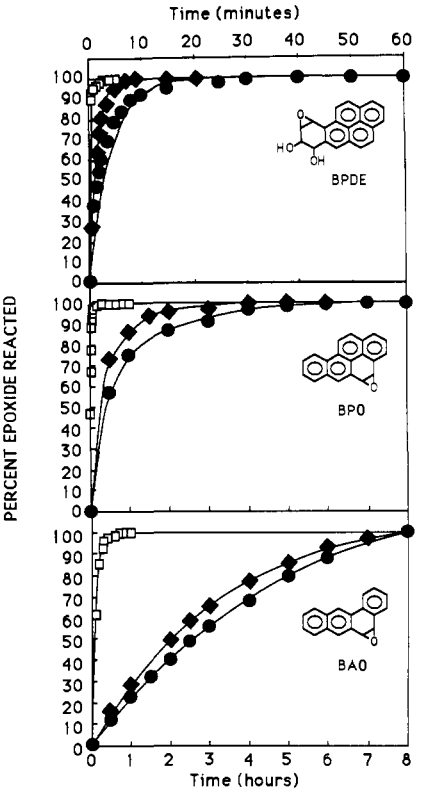

Figure 4. Results of kinetic measurements of overall, pseudo-first-order rate constants for reactions of BPDE, BAO, and BPO in calf thymus DNA. Data are given for reactions carried out in native DNA (□), in denatured DNA (♦), and in native DNA stabilized with 0.10 mM Mg^{2+} (●). The time scale at the top refers to data for BPDE. The time scale at the bottom refers to data for BPO and BAO.

For BPDE, the pseudo-first-order rate constant obtained from the data of Table II is $(7.2 \pm 1.0) \times 10^{-4}$ s^{-1}. This value agrees with earlier results.[28-32,38] For example, in 5.0 mM sodium cacodylate (pH 7.4), the hydrolysis rate constant of BPDE is 8.8×10^{-4} s^{-1}.[31a] For BAO and BPO, no results from kinetic measurements have been previously reported.

Figure 4 shows results of kinetic measurements for reactions of BPDE, BPO, and BAO carried out in native, calf thymus DNA, in denatured DNA, and in native DNA with Mg^{2+}. Table II lists rate constants obtained from the data in Figure 4. Previous investigations have demonstrated that electrostatic effects, which stabilize native DNA, reduce association constants for the physical binding of hydrocarbon metabolites when Mg^{2+} is added.[28,29,31a,33-35] Similarly, denaturing DNA, at low ionic strength, which disrupts base-stacking interactions, also causes a reduction in the physical binding of intercalating agents such as hydrocarbon metabolites.[28,31a,33-35] For example, in 15% methanol, the association constant for the intercalation of BP78D into DNA is reduced from 6100 to 160 M^{-1} when the DNA is denatured and to 700 M^{-1} in native DNA stabilized with 1.0 mM Mg^{2+}.[34] The present results for all three epoxides are consistent with data from earlier experiments with BPDE, which indicate that rate constants in native DNA without Mg^{2+} are higher than in native DNA with Mg^{2+} or in denatured DNA.[28,29,31a]

The top and middle panels of Figure 4 show results for BPDE and BPO, respectively. For both epoxides, the data indicate that, in DNA, the fluorescence intensity rises faster than in pure buffer

(65) Okamoto, T.; Shudo, K.; Miyata, N.; Kitahara, Y.; Nagata, S. *Chem. Pharm. Bull.* **1978**, *26*, 2014.

Table III. Percentage of Reactant Epoxide Forming Adducts with Calf Thymus DNA[a]

	native DNA[b]	denatured DNA[b]	native DNA + Mg^{2+} [b,c]
BPDE	10.1 ± 3.0	9.8 ± 2.6	7.6 ± 2.1
BPO	14.9 ± 1.1	9.2 ± 0.3	11.2 ± 0.4
BAO	3.6 ± 0.4	3.2 ± 0.4	2.7 ± 0.4

[a] Measured in 1.0 mM sodium cacodylate (pH 7.1). The DNA concentration was 0.20 mM in PO_4^-. [b] Reaction time utilized was 24 h. [c] Measured at an Mg^{2+} concentration of 0.10 mM.

(Figure 3). In native DNA without Mg^{2+}, BPDE catalysis occurs and reactions take place with an overall, pseudo-first-order rate constant of approximately 0.1 s^{-1}. Under the same conditions, BPO reactions are accelerated compared to those occurring in buffer alone but remain slower than the reactions of BPDE. In native DNA without Mg^{2+}, BPO has a rate constant of $(1.2 \pm 0.2) \times 10^{-2}$ s^{-1}.

The bottom panel of Figure 4 shows data for BAO. With DNA, reactions of BAO, like reactions of BPDE and BPO, are accelerated. However, DNA accelerates BAO reactions much less efficiently than it accelerates BPDE and BPO reactions. This is demonstrated by the observation that, for all reactions run in DNA, rate constants measured for BAO are smaller than those measured for BPDE and BPO. For reactions run in native DNA, in denatured DNA, and in native DNA stabilized with Mg^{2+}, the ordering of the rate constants changes from that observed for the reactions occurring in buffer alone. With DNA, the rate constants increase in the order

$$\text{BAO} < \text{BPO} < \text{BPDE}$$

In native DNA, the ratio of the rate constants is 1/4.3/36; in denatured DNA, the ratio is 1/1.6/65; in native DNA stabilized with Mg^{2+}, the ratio is 1/2.2/51.

Adduct Yields for Reactions of BPDE, BPO, and BAO with Calf Thymus DNA. Table III lists the percentage of total BPDE, BPO, and BAO that yields DNA adducts after the reactions are completed. The results demonstrate that, for each epoxide, the greatest adduct yield occurs for reactions in native DNA without Mg^{2+}. Table III also indicates that when reactions of BPO are run to completion in native DNA and in native DNA stabilized with 0.10 mM Mg^{2+}, more adducts are formed than in reactions of BPDE run under the same conditions. In denatured DNA, the yield for BPDE is slightly higher (6.5%) than that for BPO. In all experiments, yields obtained in reactions of BAO are more than 2.7 times smaller than yields obtained in reactions of BPO or BPDE run under the same conditions.

The data for BPDE in Table III are consistent with previous results[30] indicating that, in reactions with native, calf thymus DNA in 5.0 mM sodium cacodylate (pH 7.2), 10% of the epoxide forms adducts. For BPO, earlier results[43] indicate that, in 50 mM Tris-HCl buffer (pH 7.5) and ethanol (33% by volume), 33% of the epoxide reacts with poly(G) to form adducts. Under similar conditions, 6.6 and <2% of the reacting BPO forms adducts in reactions with salmon testes DNA and with poly(A).[43]

Rate of Adduct Formation. The results in Figure 4 and Table III also provide information concerning the rate at which adducts are formed. The percentage of the total initial epoxide that forms adduct at each time t is given by

$$\%\ \text{adduct}(t) = \%\ \text{adduct}_{max} \times (1 - e^{-kt}) \qquad (1)$$

In (1), % adduct_{max} is the percent of the initial epoxide that yields adducts after completion of the reaction and k is the overall, pseudo-first-order rate constant taken from Table III.

For BPDE, use of (1) indicates that when reactions with DNA are run under any of the three conditions examined, 6–10% of the total BPDE forms adducts within 10 min after the reaction is initiated. For BPO, which forms more adducts than BPDE in reactions that are run to completion, the percentage of total epoxide that forms adducts after 10 min varies significantly, depending on the reaction conditions. For reactions run in native DNA without Mg^{2+}, 14.9% of the total BPO forms adducts after 10 min. For reactions run in denatured DNA and in native DNA with Mg^{2+}, 1.4 and 1.3% of the total epoxide forms adducts after 10 min. For reactions of BAO run in native DNA without Mg^{2+}, in denatured DNA, and in native DNA with Mg^{2+}, 2.9, 0.3, and 0.1% of the total epoxide forms adducts after 10 min.

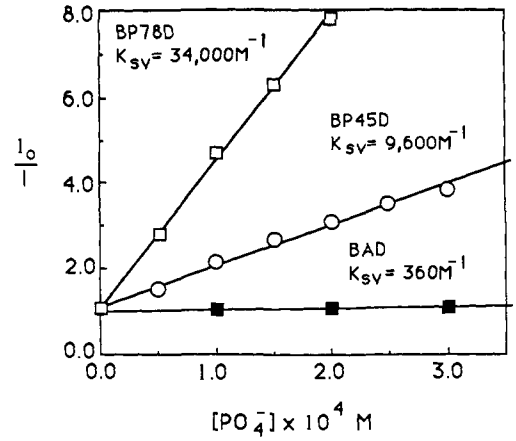

Figure 5. Stern–Volmer plots and quenching constants derived from the fluorescence quenching of *trans*-7,8-dihydroxy-7,8-dihydrobenzo[*a*]pyrene (BP78D), *trans*-4,5-dihydroxy-4,5-dihydrobenzo[*a*]pyrene (BP45D) and *cis*-5,6-dihydroxy-5,6-dihydrobenz[*a*]anthracene (BAD) by native, calf thymus DNA.

Comparison of Association Constants for the Reversible Binding of *trans*-7,8-Dihydroxy-7,8-dihydrobenzo[*a*]pyrene (BP78D), *trans*-4,5-Dihydroxy-4,5-dihydrobenzo[*a*]pyrene (BP45D), and *cis*-5,6-Dihydroxy-5,6-dihydrobenz[*a*]anthracene (BAD) to DNA. Figure 5 contains Stern–Volmer plots and quenching constants for the fluorescence quenching of the epoxide model compounds BP78D, BP45D, and BAD. The results indicate that the quenching of the diols by DNA increases in the order BAD < BP45D < BP78D. Earlier experiments[34] demonstrated that DNA influences the spectral properties of BP78D and BP45D in the same manner that it influences the properties of other aromatic hydrocarobns such as pyrene. For pyrene, intercalation into DNA leads to a red shift in the UV absorption spectrum and to fluorescence quenching.[66,67]

For systems in which dynamic quenching of the hydrocarbon by DNA is negligible and in which the fluorescence quantum yield of the intercalated complex is small compared to that of the free hydrocarbon, previous investigations[33-37] indicate that Stern–Volmer quenching constants are equal to binding constants for intercalation. When these conditions are met, the association constant for binding is given by (2).

$$K_A = K_{SV} = [\text{DNA}]^{-1}[I_0/I - 1] \qquad (2)$$

Fluorescence Lifetime Measurements. The validity of (2) has been verified by fluorescence lifetime measurements. Figure 6 shows magic angle fluorescence decay profiles for BP78D, BP45D, and BAD, measured with and without DNA. For all three diols, Figure 6 indicates that the decay profiles do not change significantly when DNA is added.

For all three diols without DNA and for BAD with DNA, the decay profiles were fit with a single-exponential decay law. In these cases, the analysis that employed a double-exponential decay law did not result in improved values of χ^2. Results from the deconvolution of the decay profiles are summarized in Figure 6, which gives lifetimes, values of χ^2, and residuals obtained in the data anlysis. For BAD, lifetimes measured with and without DNA are equal within experimental uncertainty.

(66) (a) Boyland, E.; Green, B. *Br. J. Cancer* **1962**, *16*, 347. (b) Boyland, E.; Green, B. *Br. J. Cancer* **1962**, *16*, 507.
(67) (a) Ball, J. K.; McCarter, J. A.; Smith, M. F. *Biochim. Biophys. Acta* **1965**, *103*, 275. (b) Nagata, C.; Kodama, M.; Tagashira, Y.; Imamura, A. *Biopolymers* **1966**, *4*, 409. (c) Green, B.; McCarter, J. A. *J. Mol. Biol.* **1967**, *29*, 447; (d) Craig, M.; Isenberg, I. *Biopolymers* **1970**, *9*, 689.

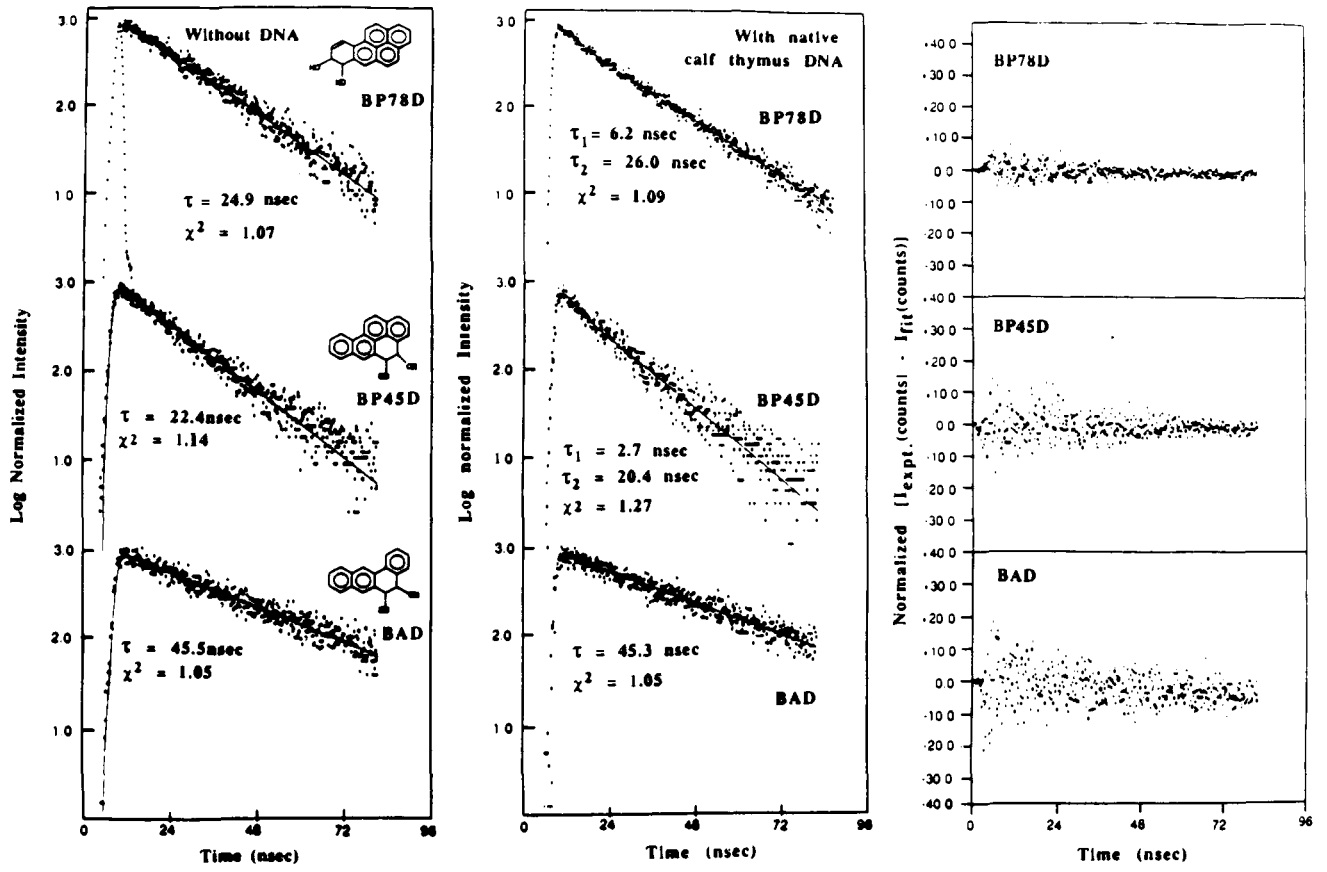

Figure 6. Magic angle fluorescence decay profiles of BP78D, BP45D, and BAD without DNA (left panel) and with native calf thymus DNA (middle panel). Fluorescence lifetimes (τ) and χ^2 values are given. The uncertainty in the reported lifetimes is ±2 ns. Measurements with DNA were carried out under conditions in which the hydrocarbon fluorescence quenching (I_0/I) was in the range 1.2–4.4. Solid lines show fits to data obtained in the deconvolution procedure. An instrument response profile is included with the decay profile in the upper left-hand corner. The panel on the right gives residuals for decay profiles measured with DNA.

Because of strong DNA quenching, lifetime data for BP78D and BP45D with DNA is of poorer quality than that for BAD or for BP78D and BP45D without DNA. Analysis of the decay profiles for BP78D and BP45D with DNA, with use of a single-exponential decay law, yielded lifetimes of 24.4 and 18.8 ns, with χ^2 values of 1.35 and 1.50, respectively. Use of a double exponential decay law improved the χ^2 values to 1.09 and 1.27. For BP78D with DNA, analysis with a double-exponential decay law yielded a short-lived component with a lifetime of 6.2 ns and a long-lived component with a lifetime equal, within experimental uncertainty, to that measured for BP78D without DNA. Similarly, for BP45D with DNA, analysis with a double-exponential decay law yielded a short-lived component (2.7 ns) and a long-lived component, with a lifetime equal to that measured for the hydrocarbon without DNA. For both BP78D and BP45D with DNA, the short-lived emission components made up less than 10% of total emission intensity. The low intensities of the short lifetime components make it difficult to determine their origin. These contributions to the total emission may arise from small errors introduced in the background subtraction procedure.

The results of the lifetime measurements indicate that the observed decay profiles of BP78D, BP45D, and BAD are not significantly altered when DNA is added. This observation is similar to that previously reported in investigations of the influence of DNA intercalation on the fluorescence decay profiles of *trans*-5,6-dihydroxy-5,6-dihydro-7,12-dimethylbenz[*a*]anthracene in aqueous solution[33] and of BP78D and BP45D in aqueous solution containing 15% methanol.[34] The data in Figure 6 support the validity of (2), indicating that the association constants are nearly equal to the Stern–Volmer quenching constants.

Table IV lists association constants for BP78D, BP45D, and BAD. The values given in the table are consistent with earlier data[34] indicating that, in 15% methanol, the association constant of BP78D is 2.8–2.9 times greater than that of BP45D. A similar difference between the association constants of bay versus K region epoxide model compounds occurs for diols derived from 7,12-dimethylbenz[*a*]anthracene.[28]

Table IV. Association Constants, Gibbs Free Energies, Enthalpies, and Entropies for the Binding of BP78D, BP45D, and BAD to Native, Calf Thymus DNA[a]

	K_A[b] (M^{-1})	ΔG (kcal/mol)	ΔH (kcal/mol)	ΔS (cal/mol deg)
BP78D[c]	$(3.4 \pm 0.1) \times 10^4$	-6.1 ± 0.1	-7.1 ± 0.5	-3.4 ± 1.5
BP45D[c]	$(9.6 \pm 0.5) \times 10^3$	-5.4 ± 0.1	-4.6 ± 0.5	2.7 ± 1.5
BAD[d]	$(3.6 \pm 0.9) \times 10^2$	-3.5 ± 0.3	-3.6 ± 0.9	-0.3 ± 3.0

[a] Measured in 1.0 mM sodium cacodylate (pH 7.1). [b] Measured at 23 °C. [c] Measured at a DNA concentration of 0.20 mM in PO_4^-. [d] Measured at a DNA concentration of 0.50 mM in PO_4^-.

Gibbs Free Energy, Enthalpy, and Entropy Changes for the Physical Binding of BP78D, BP45D, and BAD to DNA. Figure 7 shows typical data from measurements of the temperature dependence of association constants for the binding of BP78D, BP45D, and BAD to native DNA. The figure contains van't Hoff plots demonstrating how ln K_A varies with $1/T$. Table IV lists the free energy (ΔG), the enthalpy (ΔH), and the entropy (ΔS) of binding for the three diols. In Table IV, values of ΔG were obtained directly from values of the binding constants measured at 23 °C. The uncertainty in the values of K_A and ΔG, given in Table IV, are standard deviations obtained from three measurements of Stern–Volmer quenching constants. Values of ΔH and ΔS were calculated with use of the slope and intercept of an average van't Hoff plot in which all data was pooled from three measurements of ln K_A at five different temperatures.[54b] A Q test was performed on individual values of ln K_A measured at the various temperatures, and none of these individual values could be rejected at the 90% confidence level. A T_n test led to the same conclusion. The uncertainty in the values of ΔH and ΔS, given

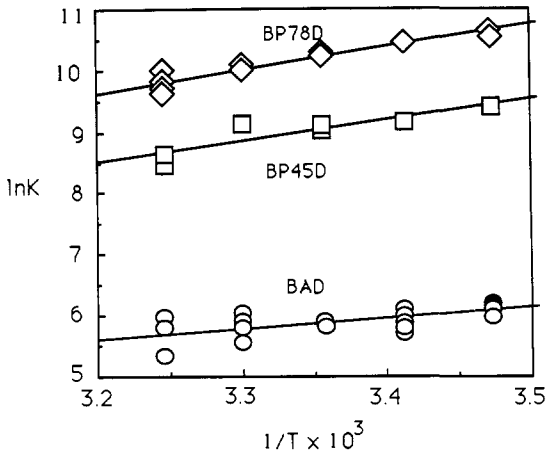

Figure 7. Van't Hoff plots showing the temperature dependence of association constants for the binding of BP78D, BP45D, and BAD to native, calf thymus DNA. Data were measured in the temperature range 15–35 °C. DNA concentrations were 0.20 mM in PO_4^- for BP78D and BP45D and 0.5 mM for BAD.

Table V. Comparison of Association Constants[a] for Binding of BPDE and BPO to Native, Calf Thymus DNA

	association constant (M^{-1})
BPDE	$(2.5 \pm 0.3) \times 10^4$
BPO	$(6.0 \pm 1.0) \times 10^3$

[a] Measured at 23 °C in 2% THF and 1.0 mM sodium cacodylate (pH 9.0).

in Table IV, are standard deviations associated with the average van't Hoff plot.[54b] Values of ΔH, which depend on the slopes of the van't Hoff plots, have greater uncertainty than the values of ΔG. For BP78D and BP45D, the uncertainty in the values of ΔH is smaller than that for BAD, because BAD binds poorly and the fluorescence intensity of BAD is weakly quenched by DNA.

The uncertainty in the values of ΔS is larger than for either ΔG or ΔH, because ΔS values are obtained by extrapolating the van't Hoff plots to high temperatures in order to evaluate the intercepts. For BAD, the large uncertainties in the ΔS values make it impossible to determine whether the sign of ΔS is positive or negative. However, the data in Table IV are in agreement with the observation that the binding of neutral ligands to polyions can result in either positive or negative entropy changes.[49,68]

Even after accounting for the uncertainty in the values of ΔS, the data in Table IV demonstrate that the difference between the values of ΔG for BP78D and BP45D has a significant enthalpic contribution. For these two diols, the difference in ΔH is the dominant factor in determining the difference in ΔG. For BAD, the uncertainty in the thermodynamic data does not permit a similar conclusion to be reached.

Comparison of Association Constants for the Reversible Binding of BPDE and BPO to DNA. To assess the validity of using model compounds to obtain the ordering of association constants for the reversible binding of BP and BA epoxides to DNA, association constants for BPDE and BPO were compared and are given in Table V.

When native DNA is added to the hydrocarbon, a loss of absorbance occurs at the wavelength (λ_{free}) of maximum absorbance. This is accompanied by an increase in the absorbance at a longer wavelength ($\lambda_{complex}$), which arises from the hydrocarbon–DNA complex.[29,47,48] The absorbance data is related[29] to the fraction of bound hydrocarbon (f_B) by (3). Here, ΔA_0 is

$$f_B = (\Delta A - \Delta A_0)/\alpha \quad (3)$$

the difference in the absorbance at λ_{free} and $\lambda_{complex}$ measured without DNA, ΔA is the difference measured with DNA, and α is a constant. The value of $1/\alpha$ has been obtained by extrapolating linear, least-squares fits of double reciprocal plots ($1/(\Delta A - \Delta A_0)$ vs $1/[DNA]$) to infinite DNA concentration, where $f_B = 1$. Association constants[29] (K_A) were obtained by using (4). Figure 8 shows plots of $1/(1 - f_B)$ versus DNA concentration. The association constants in Table V were obtained from five sets of data for both BPDE and BPO.

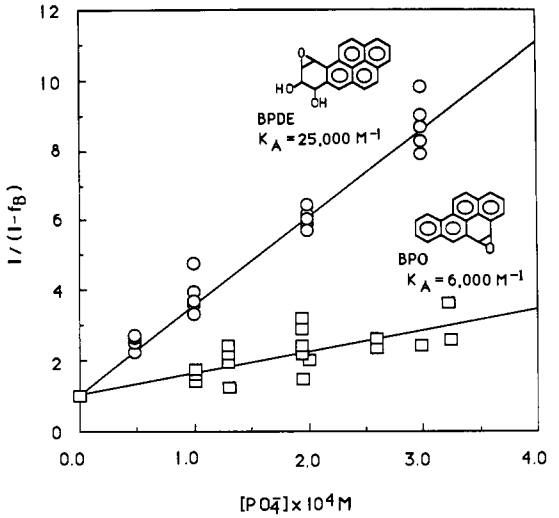

Figure 8. Results from measurements of association constants for the binding of (±)-*trans*-7,8-dihydroxy-*anti*-9,10-epoxy-7,8,9-10-tetrahydrobenzo[*a*]pyrene (BPDE) and benzo[*a*]pyrene 4,5-oxide (BPO) to native, calf thymus DNA. Data were obtained in 1.0 mM sodium cacodylate (pH 9.0).

$$1/(1 - f_B) = 1 + K_A[PO_4^-] \quad (4)$$

For BPDE, the value of K_A reported here is higher than several previously reported values,[29,31a,48] which range between 551 and 12000 M^{-1} and which were measured under a variety of conditions. However, the value given in Table V agrees well with a recently reported association constant ($(2.22 \pm 0.46) \times 10^4$ M^{-1}) of (+)-BPDE, measured in 5% ethanol and 10 mM Tris–HCl (pH 9.0).[49] The data in Table V indicate that, as predicted from results of binding experiments with the model compounds, the association constant of BPDE is greater than that of BPO.

Photoelectron Spectra of BPDE, BPO, and BAO. Figure 9 shows HeI photoelectron spectra and assignments for bands rising from the upper occupied π and oxygen atom lone-pair orbitals in BPDE, BPO, and BAO. For BPDE, the spectrum shown in Figure 9 agrees with that previously reported.[69] In the energy region 7.7–11.0 eV, the spectrum of BPDE has maxima at 7.85, 9.1, 9.78, and 10.6 eV. In the same energy region, BPO has two maxima at 8.22 and 9.14 eV and a shoulder between 10.02 and 10.4 eV. The spectrum of BAO has one resolved band at 8.16 eV and shoulders at 9.08 eV and in the range 9.4–10.0 eV. At energies above 11.0 eV, the spectra of BPDE, BPO, and BAO are poorly resolved.

The assignment of the photoelectron spectra in Figure 9 has been aided by results from ab initio SCF molecular orbital calculations that employ the STO-3G and 4-31G basis sets. Theoretical ionization potentials (IP's) have been obtained by applying Koopmans' theorem[70] to results from the SCF calculations. Figure 10 shows a comparison of experimental and theoretical IP's for BPDE and BPO. Figure 11 shows a similar comparison for BAO. Figures 10 and 11 also contain diagrams of the upper occupied orbitals, constructed from results of the 4-31G calculations. The sizes of atomic orbitals used in the molecular orbital diagrams are proportional to the molecular orbital coefficients. For p orbitals, the coefficients of the inner Gaussian terms of the 4-31G

(68) (a) Takagishi, T.; Naoi, Y.; Sonoda, I.; Kuroki, N. *J. Polym. Sci., Polym. Chem. Ed.* **1980**, *18*, 2323. (b) Shimer, G. H., Jr.; Wolfe, A. R.; Meehan, T. *Biochemistry* **1988**, *27*, 7960.

(69) Akiyama, I.; Li, K. C.; LeBreton, P. R.; Fu, P. P.; Harvey, R. G. *J. Phys. Chem.* **1979**, *83*, 2997. In this reference, the probe temperature used to measure the spectrum of BPDE was incorrectly reported to be 223 °C.

(70) Koopmans, T. *Physica* **1933**, *1*, 104.

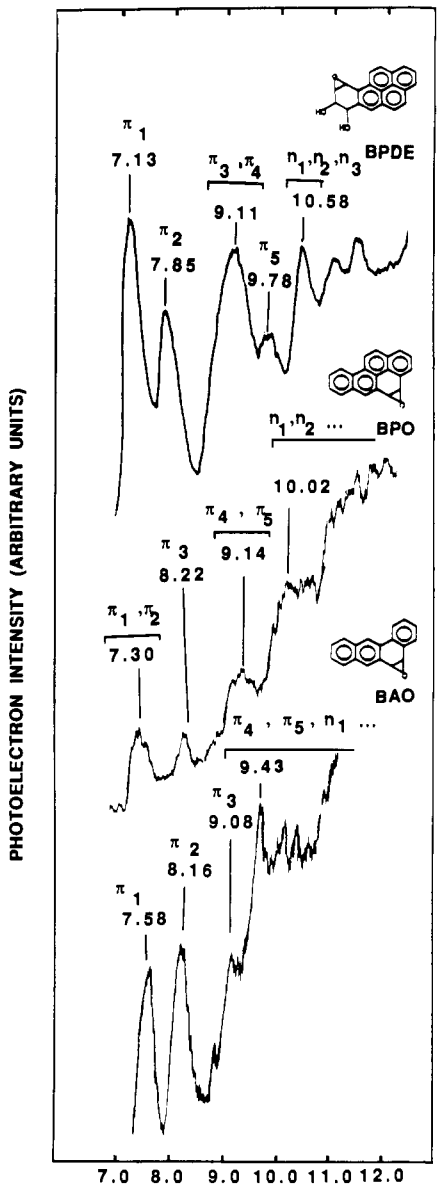

Figure 9. HeI photoelectron spectra of BPDE, BPO, and BAO along with vertical ionization potentials and assignments.

expansions were used; for s orbitals, the coefficients of the outer terms were used.[71] In each orbital diagram, all C and O, 2s and 2p contributions are shown for which orbital coefficients are greater than 0.15.

Results from the STO-3G and the 4-31G calculations indicate that the highest occupied orbitals in BPDE, BPO, and BAO are π orbitals. Both calculations agree with experiment in their prediction that, for these three molecules, the IP's decrease in the order BAO > BPO > BPDE.

Values for the IP's of the highest occupied orbitals (π_1) in BPDE, BPO, and BAO predicted by the 4-31G calculations are more accurate than values predicted by the STO-3G calculations. For the π_1 orbitals, values obtained from the 4-31G calculations agree with experimental vertical ionization potentials to within 0.2 eV. The values obtained from the STO-3G calculations are smaller than the experimental values by more than 1.5 eV. For the more tightly bound π orbitals, the theoretical IP's predicted by the STO-3G and the 4-31G calculations are of similar accuracy. For example, the IP's of the fifth highest occupied π orbitals (π_5) in BPDE, BPO, and BAO, obtained from the 4-31G calculations, are 0.4–1.4 eV larger than the experimental IP's. The IP's of the π_5 orbitals obtained from the STO-3G calculations are 0.4–0.9 eV smaller than the experimental values. While the STO-3G and the 4-31G calculations yield values of IP's that differ significantly, the energetic ordering predicted for the upper occupied orbitals is very similar in results obtained with the two basis sets. For BPDE, the only difference occurs in the character and the ordering of the π_5 orbital. According to results from the STO-3G calculations, the π_5 orbital contains significant O atom 2p contributions and has an IP that is 0.15 eV larger than that of the second highest occupied lone-pair orbital (n_2). According to the results from the 4-31G calculations, the π_5 orbital has only a small contribution from the O atom 2p orbitals and has an IP that is 0.78 eV smaller than that of the n_1 orbital.

For BPDE, the assignment in Figure 9 agrees with the 4-31G results and with an earlier assignment[69] based on results from semiempirical CNDO/S3 calculations.[72] The assignment based on 4-31G results is consistent with the observation that both the STO-3G and the 4-31G calculations indicate that the IP's of the three highest occupied lone-pair orbitals (n_1, n_2, and n_3) associated with the hydroxy and epoxy groups in BPDE differ by less than 0.70 eV. In Figure 9, the assignment of bands from these orbitals to the emission peaking at 10.6 eV is consistent with the high emission intensity observed in this energy region. The assignment in Figure 9 is also consistent with values for the lowest energy lone-pair IP's in cyclopentanol[73] and in ethylene oxide,[74] which have values of 10.21 and 10.57 eV, respectively.

For BPO and BAO, the assignment of the spectra in Figure 9 agrees with the ordering of orbitals obtained from results of both the STO-3G and 4-31G calculations. As in the case of BPDE, the results of the STO-3G calculations on BPO and BAO indicate that the lone-pair orbitals have significant contributions from C atom 2p atomic orbitals that participate in the π system. In the results from the 4-31G calculations, this mixing of the π and lone-pair orbitals is less pronounced.

Discussion

Comparison of the Intrinsic Reactivities of BPDE, BPO, and BAO. For reactions in buffer alone, the higher reactivity of the bay region diol epoxide BPDE compared to the reactivities of the K region epoxides BPO and BAO is in agreement with predictions of the *bay region theory*.[14,15,19] Further predictions of the theory were examined by comparing delocalization energies ($\Delta E_{delocal}$) for carbonium ions formed from 7,8,9,10-tetrahydrobenzo[*a*]-pyrene (THBP$^+$), 4,5-dihydrobenzo[*a*]pyrene (DHBP$^+$), and 5,6-dihydrobenz[*a*]anthracene (DHBA$^+$). These are model intermediates for reactions involving BPDE, BPO, and BAO, respectively.[14,15,19] Their structures are shown below.

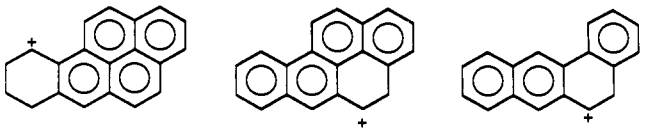

THBP$^+$ DHBP$^+$ DHBA$^+$

For these carbonium ions, $\Delta E_{delocal}$, in units of β, increases in the order DHBA$^+$ (0.575) < DHBP$^+$ (0.623) < THBP$^+$ (0.794).[14,19d,i,75] This ordering of $\Delta E_{delocal}$ does not agree with

(71) (a) Kimura, K.; Katsumata, S.; Achiba, Y.; Yamazaki, T.; Iwata, S. *Handbook of HeI Photoelectron Spectra of Fundamental Organic Molecules*; Halsted Press: New York, 1981; p 20. (b) LeBreton, P. R.; Yang, X.; Urano, S.; Fetzer, S.; Yu, M.; Leonard, N. J.; Kumar, S. *J. Am. Chem. Soc.* **1990**, *112*, 2138.

(72) (a) Lipari, N. O.; Duke, C. B. *J. Chem. Phys.* **1975**, *63*, 1748. (b) Duke, C. B.; Lipari, N. O.; Salaneck, W. R.; Schein, L. B. *J. Chem. Phys.* **1975**, *63*, 1758. (c) Lipari, N. O.; Duke, C. B. *J. Chem. Phys.* **1975**, *63*, 1768. (d) Duke, C. B.; Salaneck, W. R.; Fabish, T. J.; Ritsko, J. J.; Thomas, H. R.; Paton, A. *Phys. Rev. B: Condens. Matter* **1978**, *18*, 5717. (e) Del Bene, J.; Jaffe', H. *J. Chem. Phys.* **1968**, *48*, 4050.

(73) Tasaki, K.; Yang, X.; Urano, S.; Fetzer, S.; LeBreton, P. R. *J. Am. Chem. Soc.* **1990**, *112*, 538.

(74) (a) Schweig, A.; Thiel, W. *Chem. Phys. Lett.* **1973**, *21*, 541. (b) Corderman, R. R.; LeBreton, P. R.; Buttrill, S. E., Jr.; Williamson, A. D.; Beauchamp, J. L. *J. Chem. Phys.* **1976**, *65*, 4929. (c) McAlduff, E. J.; Houk, K. N. *Can. J. Chem.* **1977**, *55*, 318.

(75) Dewar, M. J. S. *The Molecular Orbital Theory of Organic Chemistry*; McGraw-Hill: New York, 1969; pp 214–220, 304.

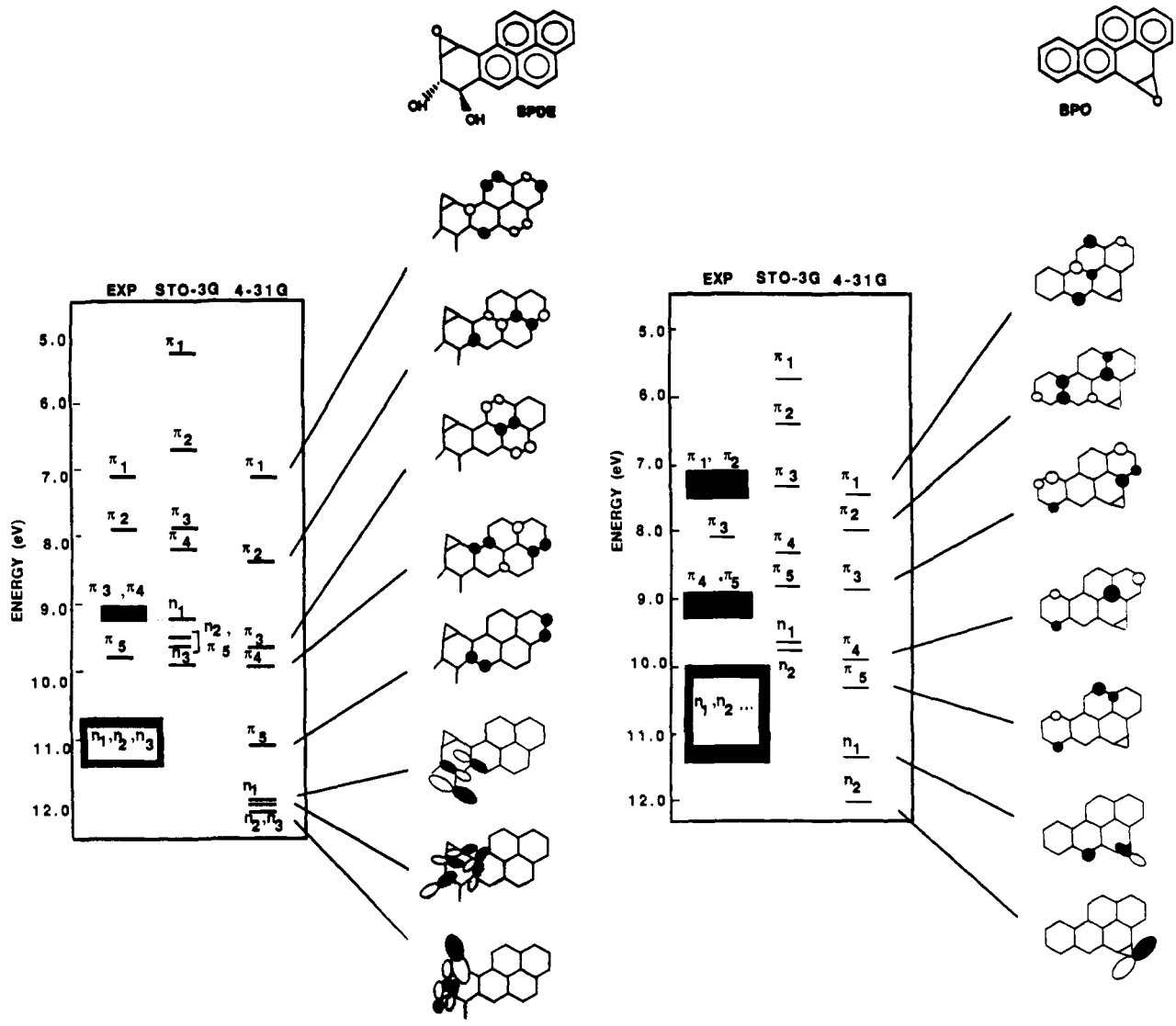

Figure 10. Energy level diagram comparing experimental and theoretical ionization potentials arising from the upper occupied molecular orbitals of BPDE and BPO. In each panel, experimental results are shown on the left. Theoretical ionization potentials obtained from the results of ab initio STO-3G calculations are shown in the middle. Ionization potentials from SCF 4-31G calculations are shown on the right. For each molecule, molecular orbital diagrams obtained from the 4-31G calculations are given.

the observation that, in buffer alone, the overall, pseudo-first-order rate constant of BAO is larger than that of BPO.

An alternate parameter that does agree with the experimental ordering of the intrinsic reactivities of BPDE, BPO, and BAO is the π electron density at benzylic carbon atoms of the protonated epoxides. This agreement is indicated by results from ab initio SCF calculations at the STO-3G level. Reactions of epoxides proceed via mechanisms with significant S_N2 character, in which the opening of the oxirane ring precedes bond formation to the incoming nucleophile.[76] Investigations[45] of the kinetics of reactions involving K region epoxides have implicated protonated structures, such as those shown below, in ring-opening, rate-determining steps leading to hydrolysis and rearrangement. For BPDE hydrolysis, protonation and ring opening occurs in a concerted fashion for general acids with pK_a's < 8.[77]

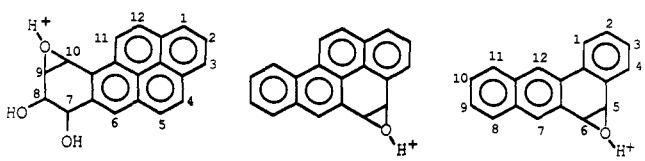

Geometries used in the STO-3G calculations on protonated BPDE, BPO, and BAO were obtained by combining geometries of the unprotonated epoxides with a 4-31G-optimized geometry of protonated ethylene oxide. Where it was possible to make comparisons, it was found that the 4-31G-optimized geometry was almost identical with an earlier reported geometry based on results from calculations with a 6-31G* basis set.[76,78]

The results of the STO-3G calculations indicate that carbon atom π electron population at the C_{10}, C_5, and C_6 atoms of protonated BPDE, BPO, and BAO, respectively, decreases in the order C_{10} (0.392) > C_6 (0.370) > C_5 (0.357). These results provide evidence that the π electron densities reflect π delocalization that occurs at benzylic carbon atoms in the protonated epoxides. Consistent with conclusions derived from calculations of $\Delta E_{\text{delocal}}$ in the carbocations, the STO-3G results predict that the π electron population at C_{10} of protonated BPDE is greater

(76) Ford, G. P.; Smith, C. T. *J. Am. Chem. Soc.* **1987**, *109*, 1325.
(77) Islam, N. B.; Gupta, S. C.; Yagi, H.; Jerina, D. M.; Whalen, D. L. *J. Am. Chem. Soc.* **1990**, *112*, 6363.

(78) The 4-31G geometry optimization of protonated ethylene oxide was carried out assuming a C_{2v} symmetry. The optimized bond lengths and bond angles from the 4-31G and the 6-31G* calculations were C–C, 1.482 Å (1.447 Å); C–O, 1.502 Å (1.498 Å); ∠OCC, 60.5° (61.1°); C–H, 1.068 Å; ∠CCH, 107.9°; O–H, 0.958 Å. For more details about the 6-31G* results (given in parentheses), see ref 76. The geometries used in the STO-3G calculations on protonated BPDE, BPO, and BAO were obtained by superimposing the plane containing the C–O–C atoms of protonated ethylene oxide on the plane containing the C–O–C atoms of the epoxide groups in neutral BPDE, BPO, and BAO.

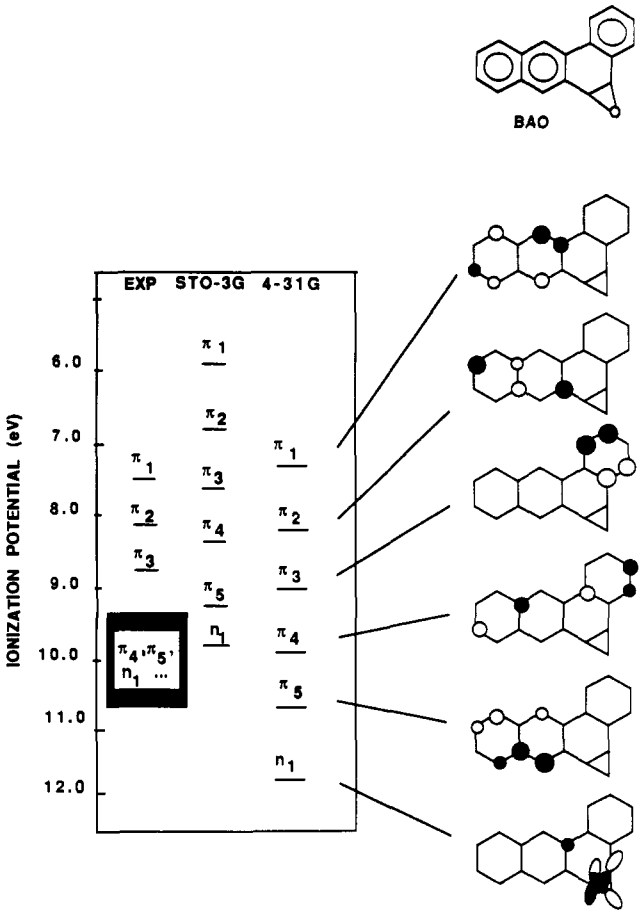

Figure 11. Energy level diagram comparing experimental and theoretical ionization potentials arising from the upper occupied molecular orbitals of BAO.

than that at C_5 of protonated BPO or at C_6 of protonated BAO. However, the STO-3G results, which predict that the π electron population at C_6 of protonated BAO is higher than that at C_5 of protonated BPO, are also consistent with the experimental observation that, in buffer alone, BAO is more reactive than BPO.

Comparison of Association Constants for the Physical Binding of BPDE, BPO, and BAO to DNA. A comparison of results from measurements of physical binding constants for the intercalation of BPDE and BPO into DNA indicates that the association constant (K_A) of BPDE is 3–6 times larger than that of BPO. This result parallels the results from the binding experiments with the model compounds, which indicate that the association constant of BP78D is 3.3–3.8 times larger than that of BP45D. The similar magnitudes of the ratio of the BPDE to BPO association constants and the ratio of the BP78D to BP45D association constants support the conclusion that the ordering of the values of K_A for the three model compounds is the same as that for the three epoxides. The observation that the value of K_A for BAD is 19 and 94 times smaller than the values for BP45D and BP78D, respectively, provides strong evidence that the association constants of the epoxides increase in the order

$$\text{BAO} < \text{BPO} < \text{BPDE}$$

Electronic Influences on the Physical Binding of BPDE to DNA. Because of the large delocalization of the hydrocarbon π systems in polycyclic hydrocarbon metabolites, such as BPDE, it is likely that polarizability plays a role in determining the enthalpic contribution to the free energy associated with the physical binding of these molecules to DNA. Hydrocarbon polarizability contributes to binding energies that rely on dipole-induced dipole interactions and on dispersion forces. The greater the polarizability, the greater is the binding energy arising from these forces. When similar molecules are compared, a decrease in ionization potential is accompanied by an increase in polarizability. Differences in the polarizabilities of BPDE, BPO, and BAO are reflected in the IP's given in Figures 9, 10, and 11. The photoelectron data indicate that the IP's of the highest occupied π orbitals increase in the order BPDE (7.13 eV) < BPO (7.30 eV) < BAO (7.58 eV). As indicated above, this is the same ordering predicted by the STO-3G and 4-31G calculations.

Table VI. Polarizabilities of Aromatic Hydrocarbons and Hydrocarbon Metabolites

	polarizability (Å^3)					
		theoretical				
molecule	STO-3G	4-31G	6-31G	4-31G*	6-31G*	experimental
benzene	4.49	7.07	7.26	7.27	7.45	10.30[a]
naphthalene	8.84	13.19	12.99	13.52		17.50[b]
anthracene	14.2	20.5	20.93			25.40[c]
BAO	17.2	25.1				
BPO	19.0					
BPDE	21.6					

[a] Taken from ref 79. [b] Taken from ref 80. [c] Taken from ref 81.

The ordering of the polarizabilities of BPDE, BPO, and BAO, predicted on the basis of IP's, agrees with theoretical polarizabilities obtained for a series of hydrocarbons from results of SCF calculations with basis sets of varying size. Table VI contains theoretical values of polarizabilities of benzene, naphthalene, anthracene, BAO, BPO, and BPDE. In cases where data are available (i.e., for benzene, naphthalene, and anthracene), Table VI also contains experimental polarizabilities.[79-81] For each molecule, calculations were carried out with use of the largest basis sets that were feasible. As the size of the molecule increases, the size of the basis set that can be employed decreases due to limited computer processing time, memory, and disk space. The results in Table VI demonstrate that the experimental values of the polarizabilities are 1.21–2.29 times larger than the calculated values and that the largest discrepancy between theory and experiment occurs for the STO-3G results. However, where comparisons are possible, the ordering of the calculated polarizabilities is the same for each of the basis sets employed.[82] Furthermore, for benzene, naphthalene, and anthracene, the ordering of the calculated polarizabilities obtained from the different basis sets agrees with the experimental ordering.

For BAO, BPO, and BPDE, the STO-3G polarizabilities in Table VI increase as the IP's of the highest occupied π orbitals decrease. Furthermore, the ordering of the STO-3G polarizabilities is the same as the ordering of the association constants for intercalation into DNA.

Comparison of the Influence of DNA on the Reactivities of BPDE, BPO, and BAO. The results of Figures 3 and 4 and Table II demonstrate that DNA influences the reactivities of BPDE, BPO, and BAO differently. Without DNA, the ordering of the overall, pseudo-first-order rate constants is BPDE > BAO > BPO. With DNA, the ordering is BPDE > BPO > BAO.

The results of the kinetic and binding measurements demonstrate that, in the presence of calf thymus DNA, the ordering of the rate constants parallels the ordering of the association constants. This suggests that the ordering of reaction rates for BPDE, BPO, and BAO in DNA is influenced as much by the ability of the epoxides to form physical complexes with DNA as it is by the intrinsic reactivities of the epoxides. The parallel between the rate constants and the association constants is consistent with the observation that, for BPDE, BPO, and BAO, overall, pseudo-first-order rate constants in DNA decrease when physical

(79) Bogaard, M. P.; Buckingham, A. D.; Corfield, M. G.; Dunmur, D. A.; White, A. H. *Chem. Phys. Lett.* **1972**, *12*, 558.
(80) Vuks, M. F. *Opt. Spectrosc. (Engl. Transl.)* **1966**, *20*, 361.
(81) Le Fèvre, R. J. W.; Radom, L.; Ritchie, G. L. D. *J. Chem. Soc. B* **1968**, 775.
(82) A comparison of the ordering of polarizabilities predicted by minimal basis set calculations (STO-3G) and by split valence basis set calculations is shown in Table VI only for hydrocarbons and not for oxygen-containing molecules. However, supplementary STO-3G, 4-31G, and 6-31G calculations were carried out on *trans*-1,2-dihydroxy-1,2-dihydroanthracene and on *trans*-1,2-dihydroxy-1,2-dihydronaphthalene. Results from calculations with all three of the basis sets indicate that, as expected, the polarizability of the anthracene diol is larger than that of the naphthalene diol.

binding is reduced by denaturing the DNA or by adding Mg^{2+}. For BPDE in denatured DNA and in native DNA stabilized with Mg^{2+}, the overall, pseudo-first-order rate constants are 8.3–50 times smaller than the rate constants measured in native DNA without Mg^{2+}. For BPO, they are 29 and 100 times smaller. For BAO, they are 14 and 33 times smaller. Like the parallel between the rate constants and the association constants, the results indicating that the rate constants measured in denatured DNA and in native DNA stabilized with Mg^{2+} are smaller than the rate constants measured in native DNA without Mg^{2+} support the conclusion that physical binding plays a key role in determining the overall reactivities of aromatic epoxides in systems containing DNA.

Comparison of the Abilities of BPDE, BPO, and BAO to Form DNA Adducts. Previous investigations have indicated that the genotoxic activity of DNA-alkylating agents sometimes correlates with the abilities of these molecules to modify DNA.[83] However, the data in Table III indicate that, in reactions with native DNA that are run to completion, BPO forms higher levels of adducts than does BPDE. For reactions in native DNA without Mg^{2+}, 14.9% of the BPO forms adducts. Under the same conditions, 10.1% of the BPDE forms adducts. For reactions in native DNA with 0.10 mM Mg^{2+}, 11.2% of the BPO and 7.6% of the BPDE forms adducts.

Interestingly, the kinetics of reactions of BPO that yield adducts exhibit much higher sensitivity to reaction conditions than do the reactions of BPDE. At short reaction times, this sensitivity can significantly alter the relative amounts of adducts formed from the three metabolites. For example, after 10 min, reactions of BPDE run in denatured DNA and in native DNA stabilized with Mg^{2+} yield 9.8 and 7.1% adducts, respectively, while reactions of BPO yield only 1.4 and 1.3% adducts.

The rate at which BAO adduct formation occurs also exhibits high sensitivity to reaction conditions. After 10 min, reactions of BAO run in native DNA without Mg^{2+} yield 2.9% adducts, while reactions in denatured DNA or in native DNA with Mg^{2+} yield only 0.3 and 0.1% adducts.

The larger overall, pseudo-first-order rate constant of BPDE in DNA stabilized with Mg^{2+}, compared to the rate constants for reactions of BPO and BAO, run under the same conditions, may contribute to the higher genotoxic activity of BPDE, compared to that of BPO or BAO. In cells, DNA is stabilized by millimolar concentrations of Mg^{2+} and polyamines,[84] and pathways by which reactive metabolites of polycyclic aromatic hydrocarbons modify DNA compete with detoxification pathways.[21-23] In the present experiments, reactions run in Mg^{2+} mimic this physiological environment better than reactions run without Mg^{2+}. The observation that, in reactions with stabilized DNA run at short reaction times, BPDE yields 5.6 and 49 times more adducts than BPO or BAO, combined with the observation that BPO and BAO are better substrates for detoxifying enzymes than BPDE, may be important for understanding the high genotoxic potency of BPDE compared to the low potency of BPO and BAO.[13,16b,c]

Acknowledgment. Support of this work by the Petroleum Research Fund, administered by the American Chemical Society (Grant No. 21314-AC), The National Cancer Institute of the National Institutes of Health (Grant No. CA41432), The American Cancer Society (Grant No. CN-37), and Cray Research, Inc., is gratefully acknowledged. Computer access time has been provided by the Computer Center of the University of Illinois at Chicago, the Cornell National Supercomputer Facility, and the National Center for Supercomputing Applications at the University of Illinois at Urbana–Champaign. A.V.B. has been supported by a Petroleum Research Fund Summer Faculty Research Fellowship. We thank Prof. Robert Moriarty, Dr. Kenzabu Tasaki, and Mr. Mark Domroese for technical assistance.

(83) (a) Brookes, P.; Lawley, P. D. *Nature* **1964**, *202*, 781. (b) Duncan, M. E.; Brookes, P.; Dipple, A. *Int. J. Cancer* **1969**, *4*, 813.

(84) (a) Hughes, M. N. *The Inorganic Chemistry of Biological Processes*; John Wiley: New York, 1981; p 258. (b) Cohen, S. S. *Introduction to the Polyamines*; Prentice Hall: Englewood Cliffs, NJ, 1971; pp 29–31.

Oxidative Photofragmentation of α,β-Amino Alcohols via Single Electron Transfer: Cooperative Reactivity of Donor and Acceptor Ion Radicals in Photogenerated Contact Radical Ion Pairs

Xiaohong Ci, Matthew A. Kellett, and David G. Whitten*

Contribution from the Department of Chemistry, University of Rochester, Rochester, New York 14627. *Received May 18, 1990. Revised Manuscript Received January 15, 1991*

Abstract: The studies presented in this paper show that α,β-amino alcohols undergo a very clean C–C bond cleavage upon SET (single electron transfer) oxidation by photoexcited electron acceptors in a process which generally culminates in two-electron reduction of the acceptors. For a number of different α,β-amino alcohols, the oxidative fragmentation occurs in a high chemical yield (>90%), yet with low to medium quantum efficiencies (0.0001–0.1) which vary strongly depending on the properties of electron donor (D), acceptor (A), and solvent. The net quantum efficiency reflects the competition between back electron transfer and the chemical redox process. Detailed mechanistic studies were carried out to investigate the visible light induced oxidative fragmentation of α,β-amino alcohols in the presence of electron acceptors including thioindigo (TI), 9,10-dicyanoanthracene (DCA), 2,6,9,10-tetracyanoanthracene (TCA), and 1,4-dicyanonaphthalene (DCN). Cosensitized (biphenyl) photoredox leads to free ions, A^- and D^+, and moderately efficient unassisted fragmentation of D^+. Quenching of $^1A^*$ by electron donor (D) to give a solvent separated radical ion pair (SSRIP) leads to a very inefficient reaction. In contrast, quenching to give a contact radical ion pair (CRIP) gives a relatively efficient reaction. This reaction is sensitive to the stereochemistry of the amino alcohol, suggesting a preferred anticoplanar configuration during the C–C bond cleavage process. The critical matching of reactivity of acceptor and donor ion radicals allows a rapid reaction to occur in the relatively narrow time window between formation and decay of the contact radical ion pair.

Introduction

Photoinduced electron-transfer reactions have been the topic of widespread recent investigation. On the one hand, a number of studies have indicated that single electron transfer (SET) quenching of excited states is a very general phenomenon which can mechanistically unify a diverse array of previously reported

0002-7863/91/1513-3893$02.50/0